Phase III. Basolateral export pumps

Cholestatic liver injury results in reversal of the secretory polarity of the hepatocyte. This phenomenon causes adaptive upregulation of transporters on the basolateral membrane that now function to facilitate the extrusion of bile salts and organic solutes by an alternate pathway, back into the hepatic sinusoids where they can be eliminated in the urine.

Multidrug resistance-associated protein 3

Multidrug resistance-associated protein 3 (MRP3: ABCC3) is localized at the basolateral membrane of hepatocytes and cholangiocytes. MRP3 has a particularly high affinity for glucuronidated conjugates and may provide the means by which bilirubin glucuronide is excreted into the blood. Hepatic MRP3 expression is increased in patients with Dubin-Johnson syndrome. This response may be viewed as a protective adaptation in situations where MRP2 function is impaired. In PBC, the expression level of MRP3 is increased (Figs 2,3).[9,39,51] Human MRP3 expression is repressed by retinoic X receptor α:retinoic acid receptor α (RXRα:RARα), which occupies specificity protein 1 activator sites in the MRP3 promoter.[52]

Multidrug resistance-associated protein 4

Multidrug resistance-associated protein 4 (MRP4: ABCC4) is an ATP-dependent organic-anion transporter with broad substrate specificity. MRP4 functions as an efflux pump for bile acids together with glutathione. MRP4 mRNA and protein levels are elevated in patients with PBC[38,39] and obstructive cholestasis[53] and in rats after bile duct ligation.[54] In PBC patients, hepatic MRP4 protein levels are increased, while MRP4 mRNA levels remained unchanged (Figs 2,3).[26]

Organic solute transporter α-β

No diseases, mutations or polymorphisms have been reported as associated with the organic solute transporter α-β (OSTα-OSTβ). OSTα-OSTβ is weakly expressed in normal liver and cholangiocytes, but highly overexpressed on the basolateral membranes of hepatocytes in cholestasis. The upregulation of basolateral efflux transporters can be viewed as adaptive responses that retard the accumulation of bile acids and other potentially toxic substrates. Hepatic levels of bile acids and other constituents of bile still continue to accumulate in the cholestatic liver and are primary substrates for the apical canalicular membrane efflux pumps. OSTα-OSTβ mRNA levels are upregulated in patients with early and late-stage PBC (Figs 2,3).[39,55]

MRP3, MRP4, and OSTα-OSTβ transporters are present in the basolateral membrane at low levels in normal liver, and are substantially overexpressed in cholestatic disorders such as PBC.

BCRP (breast cancer resistance protein), ABCG5/G8 (ATP-binding cassette transporter G5/G8), ABCA1 (ATP-binding cassette transporter A1), and AE2 (anion exchanger-2)

Breast cancer resistance protein The breast cancer resistance protein (BCRP; ABCG2) is expressed on the

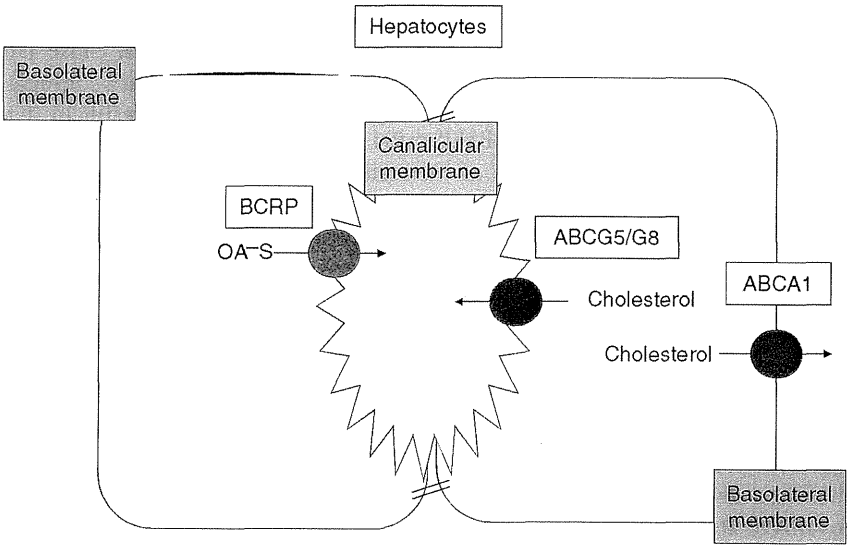

Figure 5 Hepatobiliary transporters in hepatocytes. ABCA1, ATP-binding cassette transporter A1; ABCG5/G8, ATP-binding cassette transporter G5/G8; BCRP, Breast cancer resistance protein.

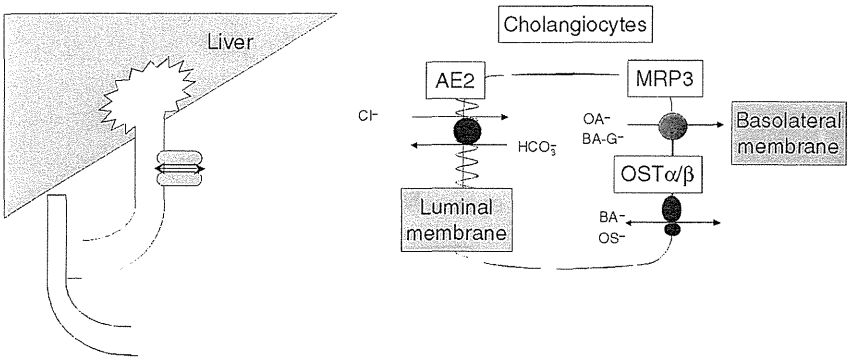

Figure 6 Hepatobiliary transporters in cholangiocytes. AE2, Anion exchanger-2; BA, bile acid; BA-G, bile acid glucuronide; MRP3, Multidrug resistance associated protein 3; OA, organic anion; OS, organic solute; OSTα-β, Organic solute transporter α-β.

canalicular membrane (Fig. 5). BCRP functions as a xenobiotic transporter that may play a role in multidrug resistance to chemotherapeutic agents, including mitoxantrone and camptothecin analogs. BCRP has been increasingly recognized for its important role in the absorption, elimination, and tissue distribution of drugs and xenobiotics. BCRP is capable of transporting non-chemotherapy drugs and xenobiotics as well, including nitrofurantoin, prazosin, glyburide, and 2-amino-1-methyl-6-phenylimidazo [4,5-b] pyridine.[56] BCRP protein levels are increased in PBC patients,[38,57] but the role of BCRP in cholestasis is unclear. In BCRP knockout mice, BCRP does not have a significant role in the adaptive response to cholestasis in the liver.[58]

ATP-binding cassette transporter G5/G8 Sterolin 1 and 2 (ABCG5/G8) are 2 ABC transporters that form a heterodimer at the canalicular membrane and account largely for the excretion of cholesterol and plant sterols (Fig. 5). Little is known about their role in cholestasis. The levels of hepatic ABCG5 mRNA and its activator, hepatic liver X receptor, are increased in the early stage of PBC.[45]

ATP-binding cassette transporter A1 The hepatic ATP-binding cassette transporter A1 (ABCA1) is localized at the basolateral membrane of hepatocytes (Fig. 5). ABCA1 is involved in exporting cholesterol from hepatocytes and is regulated in liver cells. Hepatic ABCA1 mRNA is overexpressed in patients with PBC.[59] Increased expression of ABCA1 in these patients would be expected to contribute to the hypercholesterolemia that develops during cholestasis.

Anion exchanger 2 This transporter is the canalicular Cl^-/HCO_3^- exchanger that regulates the excretion of bicarbonate. Anion exchanger 2 (AE2: SLC4A2) is also expressed on the luminal membrane of the cholangiocyte and is a determinant of bicarbonate excretion from the epithelium (Fig. 6). Hepatic AE2 mRNA expression levels are reduced in PBC patients.[60] Treatment of patients with UDCA has reportedly normalized the expression of AE2 mRNA and partially restored protein expression levels.[61] Bile salt reabsorption by cholangiocytes may contribute in part to the accumulation of bile salts and generation of hypercholeretic bile flow. Although this pathway probably plays a minor role under normal physiological conditions, cholehepatic shunting of bile salts may become an important escape route for bile salts under cholestatic conditions when the bile duct epithelium proliferates.

Intestinal and renal transporters (Fig. 7)

Cholestasis results in intrahepatic accumulation of bile acids. Intrahepatic bile acids can be detoxified via phase I hydroxylation and phase II conjugation reactions mediated by cytochrome p450 enzymes, glucuronidases, and sulfatases. These modifications render intrahepatic bile acids more hydrophilic and facilitate their elimination. Export of bile acids in cholestasis is enhanced by upregulation of hepatic basolateral adaptive overflow transporters such as MRP3, MRP4, and OSTα/β (Figs 2,3). Hydrophilic bile acids can then be eliminated by the kidney either via glomerular filtration or potentially through additional active ATP-transporters such as MRP2- and MRP4-mediated tubular secretion. In addition, reduced intestinal bile acid uptake due to reduced expression of apical sodium-dependent bile acid transporter (ASBT: SLC10A2) reduces systemic bile acid accumulation by enhancing fecal excretion of bile acids.[62,63]

CONCLUSIONS

EXPRESSION LEVELS OF hepatobiliary transporters are abnormal in patients with PBC; this is true in both early and late stages of the disease, with or without

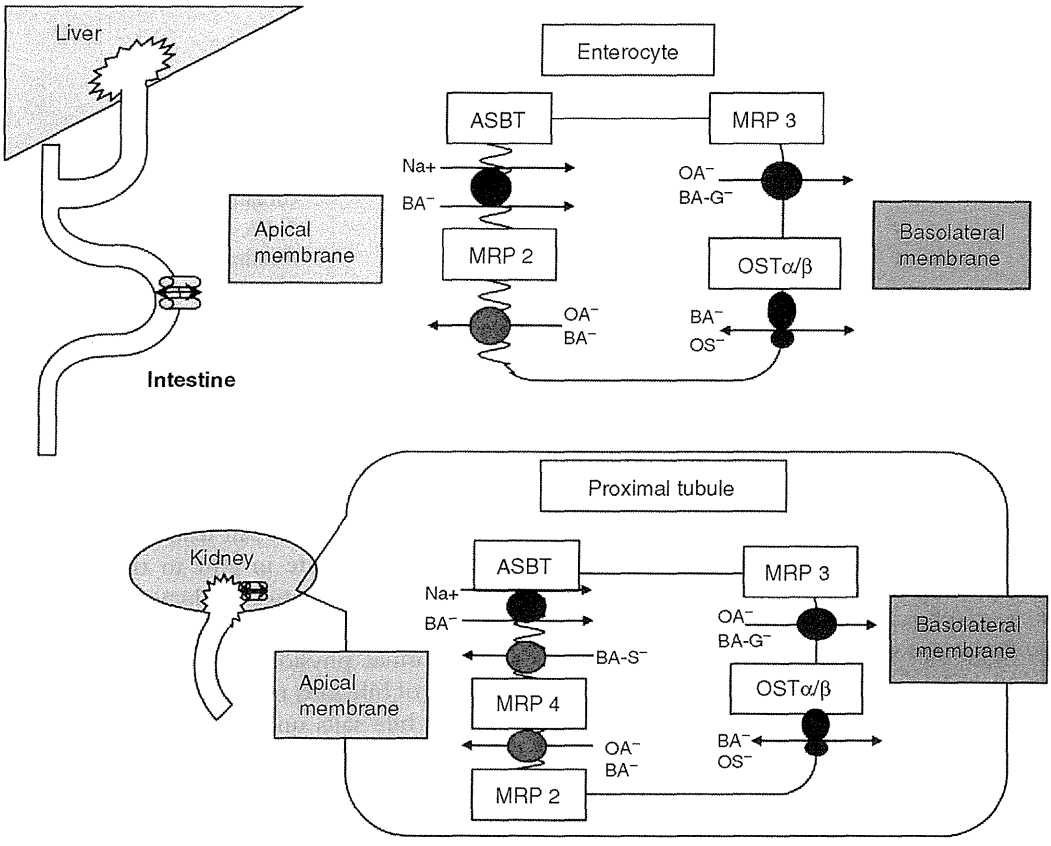

Figure 7 Intestinal and renal transporters. ASBT, apical sodium-dependent bile acid transporter; BA, bile acids; BA-G, bile acid glucuronide; BA-S, sulfated bile acid; MRP2, Multidrug resistance-associated protein 2; MRP3, Multidrug resistance-associated protein 3; MRP4, Multidrug resistance-associated protein 4; OA, organic anion; OS, organic solute; OSTα-β, Organic solute transporter α-β.

medication. Hepatobiliary transporter expression is altered in PBC, preventing the accumulation of toxic bile acids in hepatocytes. Early-stage PBC is characterized by more ductular proliferation than ductopenia, while late-stage PBC is characterized by more ductopenia than ductular proliferation. The characteristic features from early to late stage being progress of PBC disease. In late-stage PBC, the cessation of altered hepatobiliary transporter expression leads to the deterioration seen in advanced PBC disease.

Recently, FXR agonists have been used for the treatment of PBC. Nuclear receptors play roles in the transcriptional regulation of bile acid homeostasis. Six-ethyl chenodeoxycholic acid is a novel derivative of the primary human bile acid, chenodeoxycholic acid (CDCA). FXR is activated by bile salts with the rank order of potency CDCA > deoxycholate = lithocholate > cholate; 6-ethyl chenodeoxycholic acid is 100 times more potent than CDCA as an FXR agonist. This FXR agonist has been shown to lead to biochemical improvement with acceptable side effects in PBC patients who were already receiving UDCA and had baseline ALP values still above at least 1.5 times the upper limit of normal.[64] Further studies are required to establish the feasibility of FXR agonists, which hold much promise for the management of PBC.

ACKNOWLEDGMENTS

THIS WORK WAS supported partially by the Research Program of Intractable Disease provided by the Ministry of Health, Labor, and Welfare of Japan. We would like to express our gratitude to James Lorenzen Boyer, MD, Ensign Professor of Medicine and Emeritus Director, Yale Liver Center, Yale University School of Medicine.

REFERENCES

1 Kosters A, Karpen SJ. Bile acid transporters in health and disease. *Xenobiotica* 2008; **38**: 1043–71.
2 Koga H, Sakisaka S, Ohishi M, Sata M, Tanikawa K. Nuclear DNA fragmentation and expression of Bcl-2 in primary biliary cirrhosis. *Hepatology* 1997; **25**: 1077–84.
3 Harada K, Ozaki S, Gershwin ME, Nakanuma Y. Enhanced apoptosis relates to bile duct loss in primary biliary cirrhosis. *Hepatology* 1997; **26**: 1399–405.
4 Sakisaka S, Kawaguchi T, Taniguchi E *et al.* Alterations in tight junctions differ between primary biliary cirrhosis and primary sclerosing cholangitis. *Hepatology* 2001; **33**: 1460–8.
5 Sakisaka S, Koga H, Sasatomi K *et al.* Ursodeoxycholic acid reduces expression of heat shock proteins in primary biliary cirrhosis. *Liver* 2000; **20**: 78–87.
6 Suzuki N, Irie M, Iwata K *et al.* Altered expression of alkaline phosphatase (ALP) in the liver of primary biliary cirrhosis (PBC) patients. *Hepatol Res* 2006; **35**: 37–44.
7 Boyer JL. Nuclear receptor ligands: rational and effective therapy for chronic cholestatic liver disease? *Gastroenterology* 2005; **129**: 735–40.
8 Trauner M, Meier PJ, Boyer JL. Molecular pathogenesis of cholestasis. *N Engl J Med* 1998; **339**: 1217–27.
9 Zollner G, Fickert P, Silbert D *et al.* Adaptive changes in hepatobiliary transporter expression in primary biliary cirrhosis. *J Hepatol* 2003; **38**: 717–27.
10 Kullak-Ublick GA, Beuers U, Fahney C, Hagenbuch B, Meier PJ, Paumgartner G. Identification and functional characterization of the promoter region of the human organic anion transporting polypeptide gene. *Hepatology* 1997; **26**: 991–7.
11 Jung D, Podvinec M, Meyer UA *et al.* Human organic anion transporting polypeptide 8 promoter is transactivated by the farnesoid X receptor/bile acid receptor. *Gastroenterology* 2002; **122**: 1954–66.
12 Oswald M, Kullak-Ublick GA, Paumgartner G, Beuers U. Expression of hepatic transporters OATP-C and MRP2 in primary sclerosing cholangitis. *Liver* 2001; **21**: 247–53.
13 Jung D, Kullak-Ublick GA. Hepatocyte nuclear factor 1 alpha: a key mediator of the effect of bile acids on gene expression. *Hepatology* 2003; **37**: 622–31.
14 Geier A, Martin IV, Dietrich CG *et al.* Hepatocyte nuclear factor-4alpha is a central transactivator of the mouse Ntcp gene. *Am J Physiol Gastrointest Liver Physiol* 2008; **295**: G226–233.
15 Eloranta JJ, Jung D, Kullak-Ublick GA. The human Na+-taurocholate cotransporting polypeptide gene is activated by glucocorticoid receptor and peroxisome proliferator-activated receptor-gamma coactivator-1alpha, and suppressed by bile acids via a small heterodimer partner-dependent mechanism. *Mol Endocrinol* 2006; **20**: 65–79.
16 Shefer S, Hauser S, Bekersky I, Mosbach EH. Biochemical site of regulation of bile acid biosynthesis in the rat. *J Lipid Res* 1970; **11**: 404–11.
17 Chawla A, Saez E, Evans RM. Don't know much bile-ology. *Cell* 2000; **29** (103): 1–4.
18 Takeyama Y, Kanegae K, Inomata S *et al.* Sustained upregulation of sodium taurocholate cotransporting polypeptide and bile salt export pump and downregulation of cholesterol 7alpha-hydroxylase in the liver of patients with end-stage primary biliary cirrhosis. *Med Mol Morphol* 2010; **43**: 134–8.
19 Goodwin B, Jones SA, Price RR *et al.* A regulatory cascade of the nuclear receptors FXR, SHP-1, and LRH-1 represses bile acid biosynthesis. *Mol Cell* 2000; **6**: 517–26.
20 Xie W, Radominska-Pandya A, Shi Y *et al.* An essential role for nuclear receptors SXR/PXR in detoxification of cholestatic bile acids. *Proc Natl Acad Sci USA* 2001; **98**: 3375–80.
21 Marschall HU, Wagner M, Bodin K *et al.* Fxr(-/-) mice adapt to biliary obstruction by enhanced phase I detoxification and renal elimination of bile acids. *J Lipid Res* 2006; **47**: 582–92.
22 Saini SP, Sonoda J, Xu L *et al.* A novel constitutive androstane receptor-mediated and CYP3A-independent pathway of bile acid detoxification. *Mol Pharmacol* 2004; **65**: 292–300.
23 Stedman C, Robertson G, Coulter S, Liddle C. Feed-forward regulation of bile acid detoxification by CYP3A4: studies in humanized transgenic mice. *J Biol Chem* 2004; **279**: 11336–43.
24 Chen YH, Hong IC, Kuo KK, Hsu HK, Hsu C. Role of retinoid-X receptor-alpha in the suppression of rat bile acid coenzyme A-amino acid N-acyltransferase in liver during sepsis. *Shock* 2007; **28**: 65–70.
25 Miyata M, Matsuda Y, Tsuchiya H *et al.* Chenodeoxycholic acid-mediated activation of the farnesoid X receptor negatively regulates hydroxysteroid sulfotransferase. *Drug Metab Pharmacokinet* 2006; **21**: 315–23.
26 Zollner G, Wagner M, Fickert P *et al.* Expression of bile acid synthesis and detoxification enzymes and the alternative bile acid efflux pump MRP4 in patients with primary biliary cirrhosis. *Liver Int* 2007; **27**: 920–9.
27 Boyer JL. Adaptive regulation of hepatocyte transporters in cholestasis. In: Irwin M. Arias, ed. *The Liver*. West Sussex, UK: John Wiley & Sons, Ltd, 2009; 681–702.
28 Alnouti Y. Bile acid sulfation: a pathway of bile acid elimination and detoxification. *Toxicol Sci* 2009; **108**: 225–46.
29 Miura R, Tanaka A, Takikawa H. Urinary bile acid sulfate levels in patients with primary biliary cirrhosis. *Hepatol Res* 2011; **41**: 358–63.
30 Jansen PL, Muller M. Early events in sepsis-associated cholestasis. *Gastroenterology* 1999; **116**: 486–8.
31 Keitel V, Vogt C, Haussinger D, Kubitz R. Combined mutations of canalicular transporter proteins cause severee

intrahepatic cholestasis of pregnancy. *Gastroenterology* 2006; **131**: 624–9.
32 Pauli-Magnus C, Lang T, Meier Y *et al.* Sequence analysis of bile salt export pump (ABCB11) and multidrug resistance p-glycoprotein 3 (ABCB4, MDR3) in patients with intrahepatic cholestasis of pregnancy. *Pharmacogenetics* 2004; **14**: 91–102.
33 Strautnieks SS, Bull LN, Knisely AS *et al.* A gene encoding a liver-specific ABC transporter is mutated in progressive familial intrahepatic cholestasis. *Nat Genet* 1998; **20**: 233–8.
34 Lang C, Meier Y, Stieger B *et al.* Mutations and polymorphisms in the bile salt export pump and the multidrug resistance protein 3 associated with drug-induced liver injury. *Pharmacogenet Genomics* 2007; **17**: 47–60.
35 Byrne JA, Strautnieks SS, Mieli-Vergani G, Higgins CF, Linton KJ, Thompson RJ. The human bile salt export pump: characterization of substrate specificity and identification of inhibitors. *Gastroenterology* 2002; **123**: 1649–58.
36 Funk C, Pantze M, Jehle L *et al.* Troglitazone-induced intrahepatic cholestasis by an interference with the hepatobiliary export of bile acids in male and female rats. Correlation with the gender difference in troglitazone sulfate formation and the inhibition of the canalicular bile salt export pump (Bsep) by troglitazone and troglitazone sulfate. *Toxicology* 2001; **167**: 83–98.
37 Funk C, Ponelle C, Scheuermann G, Pantze M. Cholestatic potential of troglitazone as a possible factor contributing to troglitazone-induced hepatotoxicity: *in vivo* and *in vitro* interaction at the canalicular bile salt export pump (Bsep) in the rat. *Mol Pharmacol* 2001; **59**: 627–35.
38 Barnes SN, Aleksunes LM, Augustine L *et al.* Induction of hepatobiliary efflux transporters in acetaminophen-induced acute liver failure cases. *Drug Metab Dispos* 2007; **35**: 1963–9.
39 Takeyama Y, Uehara Y, Inomata S *et al.* Alternative transporter pathways in patients with untreated early-stage and late-stage primary biliary cirrhosis. *Liver Int* 2009; **29**: 406–14.
40 Makishima M, Okamoto AY, Repa JJ *et al.* Identification of a nuclear receptor for bile acids. *Science* 1999; **284**: 1362–5.
41 Sinal CJ, Tohkin M, Miyata M, Ward JM, Lambert G, Gonzalez FJ. Targeted disruption of the nuclear receptor FXR/BAR impairs bile acid and lipid homeostasis. *Cell* 2000; **102**: 731–44.
42 Wolters H, Elzinga BM, Baller JF *et al.* Effects of bile salt flux variations on the expression of hepatic bile salt transporters *in vivo* in mice. *J Hepatol* 2002; **37**: 556–63.
43 Pauli-Magnus C, Kerb R, Fattinger K *et al.* BSEP and MDR3 haplotype structure in healthy Caucasians, primary biliary cirrhosis and primary sclerosing cholangitis. *Hepatology* 2004; **39**: 779–91.
44 Nakamuta M, Fujino T, Yada R *et al.* Therapeutic effect of bezafibrate against biliary damage: a study of phospholipid secretion via the PPARalpha-MDR3 pathway. *Int J Clin Pharmacol Ther* 2010; **48**: 22–8.
45 Enjoji M, Yada R, Fujino T *et al.* The state of cholesterol metabolism in the liver of patients with primary biliary cirrhosis: the role of MDR3 expression. *Hepatol Int* 2009; **3**: 490–6.
46 Zollner G, Fickert P, Zenz R *et al.* Hepatobiliary transporter expression in percutaneous liver biopsies of patients with cholestatic liver diseases. *Hepatology* 2001; **33**: 633–46.
47 Dumoulin FL, Reichel C, Sauerbruch T, Spengler U. Semiquantitation of intrahepatic MDR3 mRNA levels by reverse transcription/competitive polymerase chain reaction. *J Hepatol* 1997; **26**: 852–6.
48 Shoda J, Okada K, Inada Y *et al.* Bezafibrate induces multidrug-resistance P-Glycoprotein 3 expression in cultured human hepatocytes and humanized livers of chimeric mice. *Hepatol Res* 2007; **37**: 548–56.
49 Kanda T, Yokosuka O, Imazeki F, Saisho H. Bezafibrate treatment: a new medical approach for PBC patients? *J Gastroenterol* 2003; **38**: 573–8.
50 Hashimoto K, Uchiumi T, Konno T *et al.* Trafficking and functional defects by mutations of the ATP-binding domains in MRP2 in patients with Dubin-Johnson syndrome. *Hepatology* 2002; **36**: 1236–45.
51 Ros JE, Libbrecht L, Geuken M, Jansen PL, Roskams TA. High expression of MDR1, MRP1, and MRP3 in the hepatic progenitor cell compartment and hepatocytes in severe human liver disease. *J Pathol* 2003; **200**: 553–60.
52 Chen W, Cai SY, Xu S, Denson LA, Soroka CJ, Boyer JL. Nuclear receptors RXRalpha: RARalpha are repressors for human MRP3 expression. *Am J Physiol Gastrointest Liver Physiol* 2007; **292**: G1221–1227.
53 Chai J, Luo D, Wu X *et al.* Changes of organic anion transporter MRP4 and related nuclear receptors in human obstructive cholestasis. *J Gastrointest Surg* 2011; **15**: 996–1004.
54 Denk GU, Soroka CJ, Takeyama Y, Chen WS, Schuetz JD, Boyer JL. Multidrug resistance-associated protein 4 is up-regulated in liver but down-regulated in kidney in obstructive cholestasis in the rat. *J Hepatol* 2004; **40**: 585–91.
55 Boyer JL, Trauner M, Mennone A *et al.* Upregulation of a basolateral FXR-dependent bile acid efflux transporter OSTalpha-OSTbeta in cholestasis in humans and rodents. *Am J Physiol Gastrointest Liver Physiol* 2006; **290**: G1124–1130.
56 Ni Z, Bikadi Z, Rosenberg MF, Mao Q. Structure and function of the human breast cancer resistance protein (BCRP/ABCG2). *Curr Drug Metab* 2010; **11**: 603–17.
57 Vander Borght S, Libbrecht L, Katoonizadeh A *et al.* Breast cancer resistance protein (BCRP/ABCG2) is expressed by progenitor cells/reactive ductules and hepatocytes and its expression pattern is influenced by disease etiology and species type: possible functional consequences. *J Histochem Cytochem* 2006; **54**: 1051–9.

58 Mennone A, Soroka CJ, Harry KM, Boyer JL. Role of breast cancer resistance protein in the adaptive response to cholestasis. *Drug Metab Dispos* 2010; **38**: 1673–8.
59 Takeyama Y, Uehara Y, Anan A *et al.* Hepatic ABCA1 transporter is up-regulated in bile duct ligation (BDL) with LPS-treated rats and in PBC patients. *J Hepatol* 2005; **42**: 239.
60 Medina JF, Martinez A, Vazquez JJ, Prieto J. Decreased anion exchanger 2 immunoreactivity in the liver of patients with primary biliary cirrhosis. *Hepatology* 1997; **25**: 12–7.
61 Prieto J, Qian C, Garcia N, Diez J, Medina JF. Abnormal expression of anion exchanger genes in primary biliary cirrhosis. *Gastroenterology* 1993; **105**: 572–8.
62 Wagner M, Zollner G, Trauner M. New molecular insights into the mechanisms of cholestasis. *J Hepatol* 2009; **51**: 565–80.
63 Boyer JL. Cholestasis: genetic and acquired. *Semin Liver Dis* 2010; **30**: 113–5.
64 Lindor KD. Farnesoid X receptor agonists for primary biliary cirrhosis. *Curr Opin Gastroenterol* 2011; **27**: 285–8.

Cholesterol 25-hydroxylation activity of CYP3A

Akira Honda,*,†,§ Teruo Miyazaki,†,§ Tadashi Ikegami,* Junichi Iwamoto,* Tomomi Maeda, Takeshi Hirayama,* Yoshifumi Saito,* Tamio Teramoto,** and Yasushi Matsuzaki[1],*,§**

Department of Gastroenterology,* Center for Collaborative Research,† and Department of Development for Community Medicine,§ Tokyo Medical University Ibaraki Medical Center, Ibaraki 300-0395, Japan; and Department of Internal Medicine,** Teikyo University School of Medicine, Tokyo 173-8605, Japan

Abstract To date, many studies have been conducted using 25-hydroxycholesterol, which is a potent regulator of lipid metabolism. However, the origins of this oxysterol have not been entirely elucidated. Cholesterol 25-hydroxylase is one of the enzymes responsible for the metabolism of 25-hydroxycholesterol, but the expression of this enzyme is very low in humans. This oxysterol is also synthesized by sterol 27-hydroxylase (CYP27A1) and cholesterol 24-hydroxylase (CYP46A1), but it is only a minor product of these enzymes. We now report that CYP3A synthesizes a significant amount of 25-hydroxycholesterol and may participate in the regulation of lipid metabolism. Induction of CYP3A by pregnenolone-16α-carbonitrile caused the accumulation of 25-hydroxycholesterol in a cell line derived from mouse liver. Furthermore, treatment of the cells with troleandomycin, a specific inhibitor of CYP3A, significantly reduced cellular 25-hydroxycholesterol concentrations. In cells that overexpressed human recombinant CYP3A4, the activity of cholesterol 25-hydroxylation was found to be higher than that of cholesterol 4β-hydroxylation, a known marker activity of CYP3A4. In addition, 25-hydroxycholesterol concentrations in normal human sera correlated positively with the levels of 4β-hydroxycholesterol ($r = 0.650$, $P < 0.0001$, n = 78), but did not significantly correlate with the levels of 27-hydroxycholesterol or 24*S*-hydroxycholesterol. These results demonstrate the significance of CYP3A on the production of 25-hydroxycholesterol.—Honda, A., T. Miyazaki, T. Ikegami, J. Iwamoto, T. Maeda, T. Hirayama, Y. Saito, T. Teramoto, and Y. Matsuzaki. **Cholesterol 25-hydroxylation activity of CYP3A.** ***J. Lipid Res.*** **2011. 52: 1509–1516.**

Supplementary key words cerebrotendinous xanthomatosis • cholesterol 25-hydroxylase • CYP3A4 • CYP27A1 • CYP46A1 • 4β-hydroxycholesterol • 25-hydroxycholesterol • oxysterols

Oxysterols are physiological regulators of cellular cholesterol homeostasis (1). They downregulate HMG-CoA reductase (2–4), the rate-limiting enzyme in the cholesterol biosynthetic pathway, by blocking processing of the sterol-regulatory element binding protein (SREBP) by inducing binding of SREBP cleavage-activating protein to a protein called Insig (insulin-induced gene) (5, 6). Furthermore, there is growing evidence that certain oxysterols may accelerate ubiquitination and degradation of HMG-CoA reductase protein (1, 7). On the other hand, oxysterols are endogenous ligands of the nuclear receptor liver X receptor α (LXRα; NR1H3) (8–10), which modulates immune responses and regulates various metabolic pathways, including cholesterol, bile acids, FAs, and glucose (11, 12).

In in vitro experiments, 25-hydroxycholesterol is widely used as a potent inhibitor of HMG-CoA reductase or as a ligand of LXRα, but the origins of this oxysterol are not entirely clear. Enzymatic production of 25-hydroxycholesterol has been reported by microsomal cholesterol 25-hydroxylase (CH25H) (13), and the activation of Toll-like receptors, a class of proteins that play a key role in the innate immune system, markedly induces CH25H and increases 25-hydroxycholesterol concentrations in mice macrophages and sera (14, 15). In comparison with mice, however, expression of CH25H has been reported to be very low in human tissues (13). Other enzymes involved in the production of 25-hydroxycholesterol are mitochondrial sterol 27-hydroxylase (CYP27A1) (16, 17) and brain-specific microsomal cholesterol 24*S*-hydroxylase (CYP46A1) (18). In addition, nonenzymatic generation of 25-hydroxycholesterol by autoxidation of cholesterol has also been described (19).

Previously, we measured hepatic concentrations of intermediates in bile acid synthesis in *Cyp27*$^{-/-}$ mice (20). In this series of analyses, we unexpectedly found that microsomal concentrations of 25-hydroxycholesterol were

This work was supported in part by Kakenhi grants (20591309, 21790633, and 22590747) from the Japan Society for the Promotion of Science and by a grant from Health Labour Sciences Research (the intractable hepato-biliary disease study group in Japan).

Manuscript received 11 January 2011 and in revised form 2 May 2011.

Published, JLR Papers in Press, May 15, 2011
DOI 10.1194/jlr.M014084

Abbreviations: CH25H, cholesterol 25-hydroxylase; CTX, cerebrotendinous xanthomatosis; CYP27A1, sterol 27-hydroxylase; CYP46A1, cholesterol 24*S*-hydroxylase; Insig, insulin-induced gene; LXR, liver X receptor; PCN, pregnenolone-16α-carbonitrile; SREBP, sterol-regulatory element binding protein; SRM, selected reaction monitoring.

[1]To whom correspondence should be addressed.
e-mail: ymatsuzaki-gi@umin.ac.jp

significantly elevated in *Cyp27*$^{-/-}$ mice (unpublished observation). This might be caused by reduced metabolism of 25-hydroxycholesterol due to inhibition of 27-hydroxylation. However, it was also possible that 25-hydroxylation of cholesterol was stimulated by enzyme upregulation in the *Cyp27*$^{-/-}$ mice. We speculated that CYP3A was the enzyme that exhibited high cholesterol 25-hydroxylation activity because CYP3A was markedly upregulated in *Cyp27*$^{-/-}$ mice and this enzyme was known to catalyze a similar reaction, i.e., 25-hydroxylation of 5β-cholestane-3α,7α,12α-triol (21).

The CYP3A subfamily consists of monooxygenases that catalyze many reactions involved in the metabolism of xenobiotics, steroid hormones, and bile acids (22). Cholesterol is also one of the substrates for CYP3A and is believed to be mainly metabolized to 4β-hydroxycholesterol (23, 24). The present study was undertaken to prove that CYP3A catalyzes not only 4β-hydroxylation but also 25-hydroxylation of cholesterol and to show the possibility that 25-hydroxycholesterol in normal human serum originates from CYP3A4.

MATERIALS AND METHODS

Chemicals

Pregnenolone-16α-carbonitrile (PCN) and troleandomycin were purchased from Sigma-Aldrich Chemical Co. (St. Louis, MO). Cholesterol and desmosterol were obtained from Steraloids, Inc. (Newport, RI), and cholesterol was used as substrate for the enzyme assay after purification with disposable silica cartridge columns (25) to remove contaminated oxysterols. Additional reagents and solvents were of analytical grade.

Cell culture

AML12 cells, a differentiated, nontransformed hepatocyte cell line that was derived from transforming growth factor α-overexpressing transgenic mice (26) were purchased from American Type Culture Collection (Manassas, VA). Cells were seeded in 6-well plates and cultured in a 1:1 mixture of Dulbecco's modified Eagle's medium and Ham's F12 medium (Invitrogen Japan KK; Tokyo, Japan) supplemented with 0.005 mg/ml insulin, 0.005 mg/ml transferrin, 5 ng/ml selenium, 40 ng/ml dexamethasone, and 10% FBS. When the cells were subconfluent, the medium was replaced with fresh medium containing PCN, troleandomycin, or desmosterol dissolved in 1% ethanol. Although 1% ethanol in the medium had no detectable effects on cell growth, the same concentration of ethanol was also added to the control wells. Cells were incubated at 37°C in a humidified incubator containing 5% CO_2 and 95% air.

RNA measurements

Total RNA was extracted from the cells using an AllPrep RNA/protein kit (QIAGEN KK; Tokyo, Japan). Reverse transcription was performed on 1 μg of total RNA using a first-strand cDNA synthesis kit for RT-PCR (Roche Diagnostics; Mannheim, Germany). Real-time quantitative PCR was performed on cDNA aliquots with FastStart DNA Master SYBR Green I and a LightCycler (Roche). The sequences of the oligonucleotide primer pairs used to amplify mouse mRNAs are 5′-GGCAGCATTGATCCTTATG-3′ and 5′-AAGAACTCCTTGAGGGAGAC-3′ for *Cyp3a11* (NM_007818), 5′-ACACCTACTTTGAAGACCCAT-3′ and 5′-TGACAACTTTCACCTCCAT-3′ for *Cyp46a1* (NM_010010), 5′-CTTCCTGCTGACCAATGAAT-3′ and 5′-AGCTTTTAGCAGAGGCATGT-3′ for *Cyp27a1* (NM_024264), 5′-CCAGCTCCTAAGTCACGTC-3′ and 5′-CACGTCGAAGAAGGTCAG-3′ for *Ch25h* (NM_009890) and 5′-CCTGTATGCCTCTGGTCGTA-3′, and 5′-CCATCTCCTGCTCGAAGTCT-3′ for β-actin (X03672). PCR amplification began with a 10 min preincubation step at 95°C, followed by 40 cycles of denaturation at 95°C for 10 s, annealing at 62°C for 10 s, and elongation at 72°C for 16 s. The relative concentration of the PCR product derived from the target gene was calculated using LightCycler System software. A standard curve for each run was constructed by plotting the crossover point against the log concentration. The concentration of target molecules in each sample was then calculated automatically by reference to this curve ($r = -1.00$), and results were standardized to the expression of β-actin. The specificity of each PCR product was assessed by melting curve analysis.

SDS-PAGE and immunoblot analysis

Cell homogenate was resolved by SDS-PAGE on a 5–20% gradient gel (e-PAGEL; ATTO Corporation, Tokyo, Japan) and transferred to a polyvinylidene difluoride membrane (Immobilon-P; Millipore, Bedford, MA). Immunoblot analyses of mouse CYP3A, CH25H, and β-actin were conducted with goat polyclonal antibody against mouse CYP3A, goat polyclonal antibodies against human CH25H (Santa Cruz Biotechnology; Santa Cruz, CA), and mouse monoclonal anti-β-actin antibody (Sigma), respectively. The membrane was blocked for 1 h in 5% fat-free milk in TBS-T (Tris-buffered saline/0.1% Tween-20) and incubated with the primary antibody against either CYP3A (1:200 dilution), CH25H (1:200 dilution), or β-actin (1:1,000 dilution) in 5% fat-free milk in TBS-T overnight at 4°C. The blot was washed three times for 10 min in TBS-T and incubated with an HRP-conjugated donkey anti-goat IgG antibody (Santa Cruz Biotechnology) for CYP3A and CH25H or with an HRP-conjugated sheep anti-mouse IgG antibody (Amersham; Buckinghamshire, UK) for β-actin. After washing, the bands were visualized by exposure to film (Hyperfilm ECL; Amersham) with an ECL Western blotting analysis system (Amersham) according to the manufacturer's instructions. The gradient gel was calibrated with prestained molecular-weight markers (Bio-Rad Japan; Tokyo, Japan).

Sample collection from human subjects

Blood samples were collected from 78 healthy adults. After coagulation and centrifugation at 1,500 *g* for 10 min, serum samples were stored at −20°C until analysis. Informed consent was obtained from all subjects, and the experimental procedures were approved by the Teikyo University Institutional Review Board.

Determination of sterol concentrations

Sterol concentrations in cell homogenate and serum were measured using our previously described HPLC-ESI-MS/MS method (27, 28). In brief, 5 μl aliquots of serum or cell homogenate (approximately 1×10^4 cells) were incubated with stable isotope-labeled oxysterols as internal standards in 1 N ethanolic KOH at 37°C for 1 h. Sterols were extracted with *n*-hexane, derivatized to picolinyl esters, and analyzed by HPLC-ESI-MS/MS. Conventional derivatization was conducted at 80°C for 60 min, but room temperature for 30 min was chosen for the specific monopicolinyl ester formation of 25-hydroxycholesterol. Monopicolinyl 25-hydroxycholesterol exhibited $[M+Na+CH_3CN]^+$ ion as the base peak, and [picolinic acid $(C_6H_5NO_2)$+Na]$^+$ ion was observed as the most-abundant product ion under various levels of collision energy. Therefore, *m/z* 571 → 146 (25 V) and *m/z* 574 → 146 (25 V) were used as the monitoring ions and optimal

collision energy for authentic and deuterated 25-hydroxycholesterol monopicolinate, respectively. Essentially, the Hypersil GOLD column (150 mm × 2.1 mm ID, 3 μm; Thermo Fisher Scientific, San Jose, CA) was employed for the HPLC separation of sterols, and the Hypersil GOLD aQ column (150 mm × 2.1 mm ID, 3 μm) was also used to obtain better separation of the stereoisomers (29).

Enzyme assay

Microsomes (baculosomes) prepared from insect cells that were infected with a baculovirus containing the cDNA for rabbit cytochrome P450 reductase and human *CYP1A2*, *CYP2C9*, *CYP2D6*, or *CYP3A4* were purchased from Invitrogen. The microsomes (10 pmol of P450) were incubated for 30 min at 37°C with various amounts of cholesterol (dissolved in 12 μl of a 33% aqueous solution of 2-hydroxypropyl-β-cyclodextrin), NADPH (1.2 mM), glucose-6-phosphate (3.6 mM), 2 U glucose-6-phosphate dehydrogenase, and 100 mM potassium phosphate buffer (pH 7.4) containing 0.1 mM EDTA in a total volume of 0.5 ml. The incubation was stopped by the addition of 1 ml ethanol. After the addition of the internal standards and 5 μg butylated hydroxytoluene to the mixture, oxysterols were extracted twice with 2 ml *n*-hexane, derivatized to picolinyl esters, and analyzed by HPLC-ESI-MS/MS, as described above. To exclude the possible effects of contaminated oxysterols in substrate (cholesterol) and cholesterol autoxidation, incubations without adding NADPH generating system were conducted simultaneously, as a control, and the data were subtracted from those obtained using complete assay mixtures. An assay using boiled CYP3A4 was also conducted to exclude the direct effects of the NADPH generating system on cholesterol oxidation.

Statistics

Data are expressed as the mean ± SD. The statistical significance of differences between the results in the different groups was evaluated using the Student's two-tailed *t*-test. Correlation was tested by calculating Pearson's correlation coefficient, *r*. For all analyses, significance was accepted at the level of $P < 0.05$.

RESULTS

The effects of PCN, troleandomycin, and desmosterol on sterol concentrations in AML12 cells are shown in **Fig. 1**. The concentrations of 4β-hydroxycholesterol, 25-hydroxycholesterol, and 22R-hydroxycholesterol were significantly increased by treatment with PCN, a classical inducer of CYP3A by the activation of pregnane X receptor (NR1I2) (22). In contrast, these oxysterol concentrations were significantly decreased by treatment with troleandomycin, a specific inhibitor of CYP3A activity (30). Furthermore, the increase of 25-hydroxycholesterol by PCN treatment was not suppressed by the addition of desmosterol, a potent inhibitor of CH25H (13). On the other hand, significant increase by PCN was not observed regarding the other oxysterol concentrations.

The effects of PCN, troleandomycin, and desmosterol on mRNA expressions of *Cyp3a11*, *Ch25h*, *Cyp46a1*, and *Cyp27a1* in AML12 cells are shown in **Fig. 2**. Treatment with PCN significantly upregulated *Cyp3a11* expression. Marked upregulation of *Ch25h* expression was also observed in the PCN-treated cells, but the absolute mRNA expression of *Ch25h* in untreated AML12 cells was more than 50 times lower than that of *Cyp3a11* (data not shown). Troleandomycin tended to upregulate the mRNA expression of *Cyp3a11*, but the difference was not statistically significant. The addition of desmosterol to cell culture medium did not affect the induction of *Cyp3a11* by PCN. However, desmosterol seemed to inhibit the induction of *Ch25h* by PCN.

Figure 3 shows the effects of PCN, troleandomycin, and desmosterol on protein levels of CYP3A and CH25H. PCN increased CYP3A protein level, which was associated with the upregulated transcription of *Cyp3a11* (Fig. 2). However, although the transcription of *Ch25h* was also upregulated by the addition of PCN, the protein level of CH25H was not elevated. In addition, desmosterol did not affect the expression of cellular CYP3A protein, but CH25H protein level was obviously decreased by desmosterol treatment.

Intact or boiled aliquots of insect cell microsomes overexpressing recombinant human CYP3A4 (10 pmol of P450) were incubated at 37°C for 30 min with 200 μM cholesterol and an NADPH generating system, and the sterol fraction was derivatized to picolinyl esters by two different methods. **Figures 4A, C** represent selected reaction monitoring (SRM) of samples that were derivatized at 80°C for 60 min. This derivatizing method generally produced dipicolinyl esters of oxysterols, and the SRM data indicated that 25-hydroxycholesterol was a major product of intact CYP3A4, as well as 4β-hydroxycholesterol. We also derivatized the sample at room temperature for 30 min, which produced mono-picolinyl ester of 25-hydroxycholesterol (Fig. 4B, D). The mass spectrum and retention time of mono-picolinyl 25-hydroxycholesterol are completely distinct from those of di-picolinyl 25-hydroxycholesterol. The production of 25-hydroxycholesterol by intact CYP3A4 was confirmed using this specific derivatization technique.

The effects of substrate (cholesterol) concentrations on various hydroxylase activities in recombinant human CYP3A4 are presented in **Fig. 5**. The most significant activity was 25-hydroxylation, which was higher than that of 4β-hydroxylation, a marker activity of CYP3A4. Other hydroxylation activities, i.e., 22R-, 24R-, 24*S*-, 26-, and 27-hydroxylation were also observed, but the activities were much lower than that of 4β-hydroxylation. Apparent V_{max} and K_m were calculated by Lineweaver-Burk plots. V_{max} of 25-, 4β-, 22R-, 24R-, 24*S*-, 26-, and 27-hydroxylation were 7.0×10^{-4}, 2.0×10^{-4}, 5.7×10^{-5}, 5.8×10^{-5}, 3.4×10^{-6}, 5.3×10^{-5}, and 2.3×10^{-5} mol/s/mol P450, respectively, and K_m of those hydroxylations were 182, 62, 37, 161, 15, 80, and 45 μM, respectively.

In **Table 1**, cholesterol 25- and 4β-hydroxylase activities are compared among four different insect cell microsomes containing recombinant human CYP1A2, CYP2C9, CYP2D6, or CYP3A4. Not only CYP3A4 but also the other three P450 enzymes significantly catalyzed 25-hydroxylation of cholesterol, but these activities were lower than that by CYP3A4. In contrast, 4β-hydroxylation of cholesterol was exclusively observed in microsomes containing CYP3A4. Control microsomes without expressed human P450 enzymes did not convert cholesterol into 25-hydroxycholesterol or 4β-hydroxycholesterol.

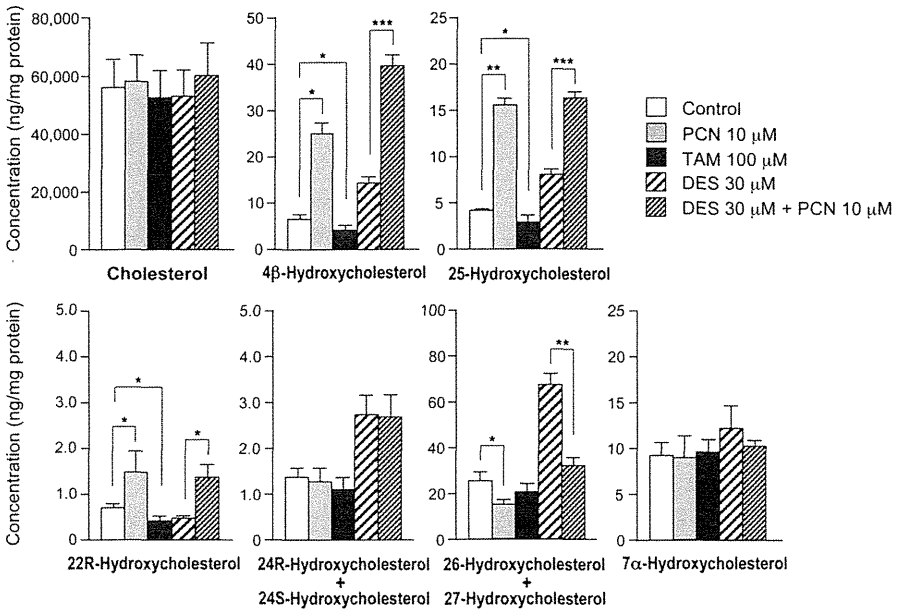

Fig. 1. Effects of PCN, troleandomycin (TAM), and desmosterol (DES) on sterol concentrations in AML12 cells. Cells were incubated with PCN (10 μM), TAM (100 μM), DES (30 μM), or DES (30 μM) plus PCN (10 μM) for 7 days. A Hypersil GOLD column was used for HPLC separation of oxysterols. This column cannot distinguish between 26- and 27-hydroxycholesterol and between 24R- and 24*S*-hydroxycholesterol. Each column and error bar represents the mean and SD obtained in triplicate assay. $***P < 0.001$, $**P < 0.01$, $*P < 0.05$.

The relationships between serum 25-hydroxycholesterol concentrations and serum 4β-, 24*S*-, and 27-hydroxycholesterol concentrations in 78 normal Japanese subjects are shown in **Fig. 6**. Serum 25-hydroxycholesterol concentrations correlated significantly with 4β-hydroxycholesterol concentrations (Fig. 6A), but did not correlate significantly with the concentrations of 24*S*-hydroxycholesterol (Fig. 6B) or 27-hydroxycholesterol (Fig. 6C). On the other hand, serum 24*S*-hydroxycholesterol and 27-hydroxycholesterol concentrations correlated significantly ($r = 0.408$, $P < 0.0005$, n = 78) in the group of normal subjects.

DISCUSSION

Our results provide strong evidence that 25-hydroxylation of cholesterol is catalyzed by CYP3A. First, CYP3A induction caused the accumulation of 25-hydroxycholesterol in a cell line derived from mouse liver. The addition of desmosterol downregulated CH25H protein in the cells, but did not reduce the concentration of cellular 25-hydroxycholesterol. Second, the presence of significant cholesterol 25-hydroxylation activity was proven by using recombinant human CYP3A4. Third, 25-hydroxycholesterol concentrations in normal human sera correlated positively with the 4β-hydroxycholesterol level; a known marker of CYP3A4 activity (23, 24).

In this study, we paid close attention to identifying 25-hydroxycholesterol by using two different derivatization methods, i.e., 80°C for 60 min and room temperature for 30 min. The former method synthesizes the usual dipicolinyl derivative of 25-hydroxycholesterol, whereas the latter method produces the mono-picolinyl derivative, because the C-25 position of 25-hydroxycholesterol is resistant to picolinyl ester formation at room temperature (28). The identification of 25-hydroxycholesterol by our conventional HPLC-MS/MS method was confirmed using

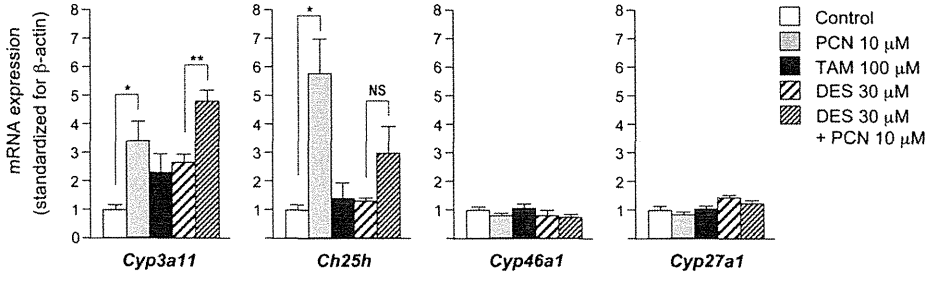

Fig. 2. Effects of PCN, troleandomycin (TAM), and desmosterol (DES) on relative mRNA expression of *Cyp3a11*, *Ch25h*, *Cyp46a1*, and *Cyp27a1* in AML12 cells. Cells were incubated with PCN (10 μM), TAM (100 μM), DES (30 μM), or DES (30 μM) plus PCN (10 μM) for 72 h. Each column and error bar represents the mean and SD obtained in triplicate assay. $**P < 0.01$, $*P < 0.05$. NS, not significant.

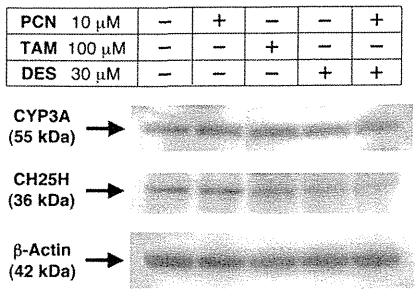

Fig. 3. Effects of PCN, troleandomycin (TAM), and desmosterol (DES) on CYP3A and CH25H protein in AML12 cells. Cells were incubated with PCN (10 μM), TAM (100 μM), DES (30 μM), or DES (30 μM) plus PCN (10 μM) for 72 h. Cell homogenates (10 μg protein per lane) were subjected to SDS-PAGE analysis.

this specific derivatization technique. Furthermore, we quantified 25-hydroxycholesterol with great care because this oxysterol may be a normal contaminant of the substrate (cholesterol) and could be generated by cholesterol autoxidation. Therefore, in the recombinant cytochrome P450 experiments, control assays without adding the NADPH generating system were conducted simultaneously and the data were subtracted from those obtained using the complete assay system.

It was surprising that recombinant CYP3A4 produced much more 25-hydroxycholesterol than 4β-hydroxycholesterol, which is used as a marker of CYP3A4 activity (23, 24). However, serum concentrations of 25-hydroxycholesterol were low compared with those of 4β-hydroxycholesterol (Fig. 6A), which may be explained by the fact that the metabolism of 25-hydroxycholesterol is faster than that of 4β-hydroxycholesterol (31). Whereas 4β-hydroxycholesterol is metabolized slowly by CYP7A1 and CYP27A1 (31), 25-hydroxycholesterol is metabolized faster by CYP7A1 (32) and CYP7B1 (33).

It has been reported that 25-hydroxycholesterol is synthesized not only by CH25H (13) but also by CYP27A1 (16, 17) and CYP46A1 (18). Because only very low levels of

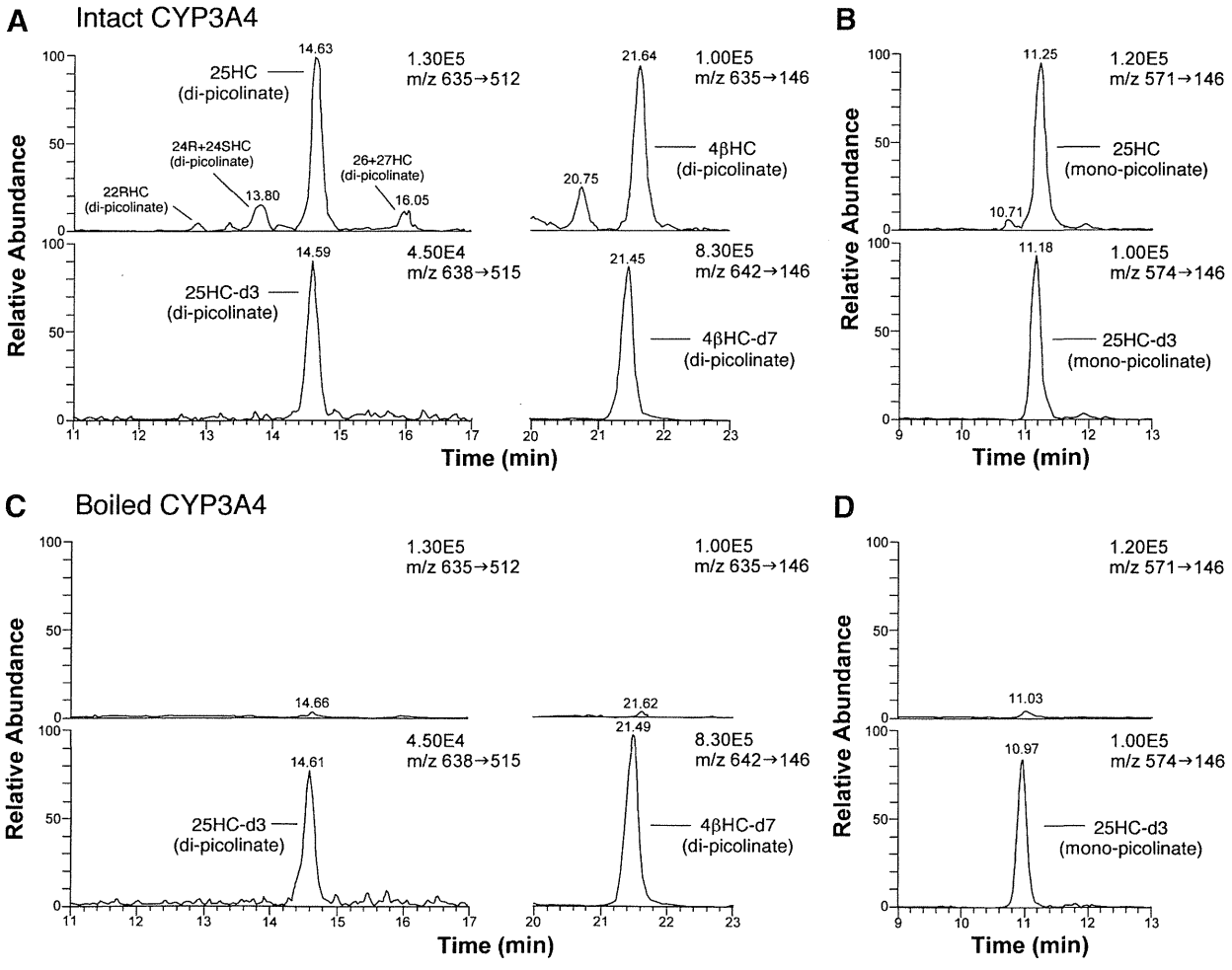

Fig. 4. SRM chromatograms obtained during HPLC-ESI-MS/MS analysis of the oxysterol fraction from an incubation mixture of overexpressed recombinant human CYP3A4 (A, B) or boiled CYP3A4 (C, D) with 200 μM cholesterol. The oxysterol fraction was derivatized to picolinyl esters by two different methods, 80°C for 60 min (A, C) and room temperature for 30 min (B, D). The former produces di-picolinyl esters of 25-hydroxycholesterol (25HC) and 4β-hydroxycholesterol (4βHC), whereas the latter produces the mono-picolinyl ester of 25HC. 25HC-d3 (1 ng) and 4βHC-d7 (5 ng) were added to each incubated mixture as internal standards. The same Hypersil GOLD column and the same mobile phase were used for HPLC separation of both di- and mono-picolinyl esters of 25HC. The numbers on the right upper side of each chromatogram represent the full scale of the chromatogram.

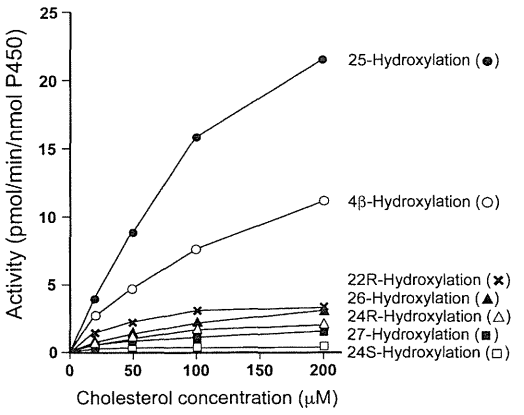

Fig. 5. Effects of cholesterol (substrate) concentrations on 25-, 4β-, 22R-, 24R-, 24*S*-, 26-, and 27-hydroxylase activities in overexpressed recombinant human CYP3A4. A Hypersil GOLD aQ column was used for HPLC separation of oxysterols. Data points represent the mean of duplicate determinations.

CH25H are expressed in normal human tissues (13), the roles of CYP27A1 and CYP46A1 in the formation of 25-hydroxycholesterol may be relatively important in humans. However, our results showed that the serum concentrations of 25-hydroxycholesterol did not correlate with the concentrations of either 27-hydroxycholesterol, a product of CYP27A1, or 24*S*-hydroxycholesterol, a product of CYP46A1. In contrast, 25-hydroxycholesterol levels were significantly correlated with 4β-hydroxycholesterol concentrations in normal human subjects. The results lend support to the hypothesis that CYP3A4 synthesizes 25-hydroxycholesterol, as well as 4β-hydroxycholesterol.

Our results showed that not only CYP3A4 but also CYP1A2, CYP2C9, and CYP2D6 catalyzed 25-hydroxylation of cholesterol to some extent (Table 1). However, CYP3A4 is the most abundantly expressed form of P450 in human liver (as much as 60% of all hepatic P450) (34). In addition, because cholesterol 4β-hydroxylase activities by CYP1A2, CYP2C9, and CYP2D6 were negligible, the positive correlation between serum concentrations of 25-hydroxycholesterol and 4β-hydroxycholesterol cannot be explained by these P450 activities. Thus, at least in normal human subjects, most of the serum 25-hydroxycholesterol appears to originate from CYP3A4.

Under abnormal conditions, however, serum 25-hydroxycholesterol concentrations may not change with 4β-hydroxycholesterol levels. For example, in a patient with cerebrotendinous xanthomatosis (CTX), *CYP27A1* deficiency, serum 25-hydroxycholesterol concentration was low but 4β-hydroxycholesterol concentration was high compared with those in a normal subject (28). Because CYP3A4 activity is not significantly altered in CTX (21), it is likely that these oxysterol concentrations were affected by the activities of other enzymes, i.e., impaired CYP27A1 and upregulated CYP7A1 (21) that metabolize 4β-hydroxycholesterol and 25-hydroxycholesterol, respectively. A recent report by Diczfalusy et al. (15) showed that intravenous injection of lipopolysaccharide (endotoxin) in healthy volunteers resulted in an increase in plasma 25-hydroxycholesterol concentration. Although CH25H activity was not determined in these subjects, the increase might be due to the induction of CH25H, as suggested by their experiments using mouse macrophage.

The biochemical role of the production of 25-hydroxycholesterol by CYP3A remains unclear. However, this oxysterol appears to be further metabolized to bile acids (35), which may be one of the important alternative pathways for bile acid biosynthesis. In addition, this oxysterol is a potent inhibitor of HMG-CoA reductase and a ligand of LXRα, so that it may participate in the regulation of lipid metabolism. It should be noted that CYP3A4 catalyzes not only 25-hydroxylation but also 4β-hydroxylation, 22R-hydroxylation, and other nonstereospecific hydroxylations of cholesterol, including 24R-, 24*S*-, 26-, and 27-hydroxylation (Fig. 5). Because 4β-hydroxycholesterol, 22R-hydroxycholesterol, and 24*S*-hydroxycholesterol have been reported to be more potent activators of LXRα compared with 25-hydroxycholesterol (8, 9), the influence of CYP3A induction on LXRα activity is not explained by the effects of 25-hydroxycholesterol alone.

Fatty liver and hypertriglyceridemia are characteristic features in *Cyp27*$^{-/-}$ mice (36) but not in CTX patients. Because CYP3A is markedly upregulated in *Cyp27*$^{-/-}$ mice but not in CTX patients (21), oxysterols synthesized by CYP3A may induce fatty liver in *Cyp27*$^{-/-}$ mice. In fact, SREBP1, a target gene of LXRα, and SREBP1-regulated FA biosynthetic enzymes were upregulated in *Cyp27*$^{-/-}$ mice (36), whereas SREBP1 was not upregulated in CTX patients (37).

TABLE 1. Cholesterol 25- and 4β-hydroxylation activities in recombinant overexpressed human cytochrome P450 (baculosomes[a])

	P450 concentration	25-Hydroxylation[b]		4β-Hydroxylation[b]	
Baculosomes	*pmol P450/mg protein*	*pmol/min/mg protein*	*pmol/min/nmol P450*	*pmol/min/mg protein*	*pmol/min/nmol P450*
WT control[c]	0	0.06 (0.07, 0.05)	—	0.01 (0.00, 0.01)	—
CYP1A2	98	0.58 (0.54. 0.62)	5.95 (5.54, 6.35)	0.12 (0.13, 0.11)	1.21 (1.30, 1.12)
CYP2C9	313	1.36 (1.50, 1.21)	4.34 (4.79, 3.89)	0.25 (0.28, 0.21)	0.79 (0.90, 0.68)
CYP2D6	252	0.59 (0.64, 0.54)	2.36 (2.56, 2.15)	0.14 (0.17, 0.10)	0.54 (0.69, 0.39)
CYP3A4	96	1.86 (2.07, 1.64)	19.4 (21.6, 17.1)	0.99 (1.08, 0.89)	10.3 (11.2, 9.31)

WT, wild type.
[a]Microsomes prepared from insect cells that were infected with baculovirus containing the cDNAs for human cytochrome P450 and rabbit cytochrome P450 reductase.
[b]Average of two assays. Individual values in parentheses.
[c]Control microsomes prepared from insect cells that were infected with a wild-type baculovirus.

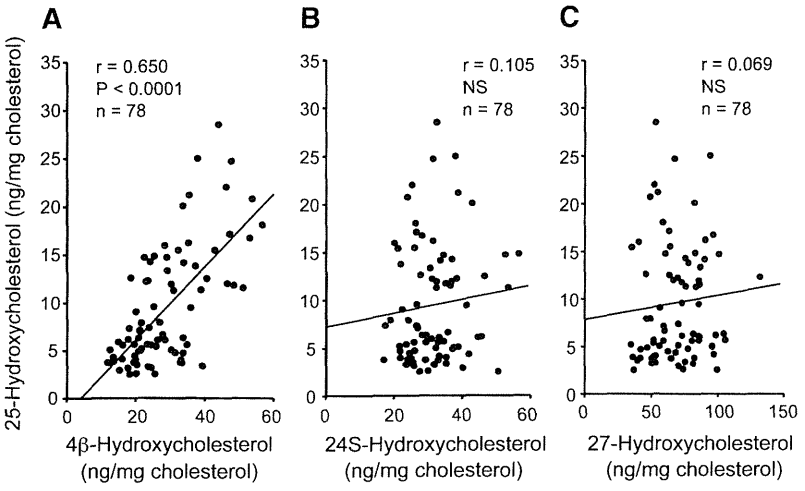

Fig. 6. Correlations between serum concentrations of 25-hydroxycholesterol and 4β-hydroxycholesterol (A), 24*S*-hydroxycholesterol (B), or 27-hydroxycholesterol (C) in 78 normal subjects. NS, not significant.

In summary, 25-hydroxycholesterol was quantified using the latest HPLC-ESI-MS/MS technique in a mouse liver cell line, in microsomes overexpressing recombinant human cytochrome P450 enzymes and in normal human sera. All data support the idea that CYP3A was one of the responsible enzymes that catalyzed the 25-hydroxylation of cholesterol.

REFERENCES

1. Gill, S., R. Chow, and A. J. Brown. 2008. Sterol regulators of cholesterol homeostasis and beyond: the oxysterol hypothesis revisited and revised. *Prog. Lipid Res.* **47:** 391–404.
2. Krieger, M., J. L. Goldstein, and M. S. Brown. 1978. Receptor-mediated uptake of low density lipoprotein reconstituted with 25-hydroxycholesteryl oleate suppresses 3-hydroxy-3-methylglutaryl-coenzyme A reductase and inhibits growth of human fibroblasts. *Proc. Natl. Acad. Sci. USA.* **75:** 5052–5056.
3. Spencer, T. A., A. K. Gayen, S. Phirwa, J. A. Nelson, F. R. Taylor, A. A. Kandutsch, and S. K. Erickson. 1985. 24(S),25-epoxycholesterol. Evidence consistent with a role in the regulation of hepatic cholesterogenesis. *J. Biol. Chem.* **260:** 13391–13394.
4. Axelson, M., and O. Larsson. 1995. Low density lipoprotein (LDL) cholesterol is converted to 27-hydroxycholesterol in human fibroblasts. *J. Biol. Chem.* **270:** 15102–15110.
5. Adams, C. M., J. Reitz, J. K. De Brabander, J. D. Feramisco, L. Li, M. S. Brown, and J. L. Goldstein. 2004. Cholesterol and 25-hydroxycholesterol inhibit activation of SREBPs by different mechanisms, both involving SCAP and Insigs. *J. Biol. Chem.* **279:** 52772–52780.
6. Radhakrishnan, A., Y. Ikeda, H. J. Kwon, M. S. Brown, and J. L. Goldstein. 2007. Sterol-regulated transport of SREBPs from endoplasmic reticulum to Golgi: oxysterols block transport by binding to Insig. *Proc. Natl. Acad. Sci. USA.* **104:** 6511–6518.
7. Goldstein, J. L., R. A. DeBose-Boyd, and M. S. Brown. 2006. Protein sensors for membrane sterols. *Cell.* **124:** 35–46.
8. Janowski, B. A., P. J. Willy, T. R. Devi, J. R. Falck, and D. J. Mangelsdorf. 1996. An oxysterol signalling pathway mediated by the nuclear receptor LXRα. *Nature.* **383:** 728–731.
9. Janowski, B. A., M. J. Grogan, S. A. Jones, G. B. Wisely, S. A. Kliewer, E. J. Corey, and D. J. Mangelsdorf. 1999. Structural requirements of ligands for the oxysterol liver X receptors LXRα and LXRβ. *Proc. Natl. Acad. Sci. USA.* **96:** 266–271.
10. Reschly, E. J., N. Ai, W. J. Welsh, S. Ekins, L. R. Hagey, and M. D. Krasowski. 2008. Ligand specificity and evolution of liver X receptors. *J. Steroid Biochem. Mol. Biol.* **110:** 83–94.
11. Wojcicka, G., A. Jamroz-Wisniewska, K. Horoszewicz, and J. Beltowski. 2007. Liver X receptors (LXRs). Part I: structure, function, regulation of activity, and role in lipid metabolism. *Postepy Hig. Med. Dosw. (Online).* **61:** 736–759.
12. Jamroz-Wisniewska, A., G. Wojcicka, K. Horoszewicz, and J. Beltowski. 2007. Liver X receptors (LXRs). Part II: non-lipid effects, role in pathology, and therapeutic implications. *Postepy Hig. Med. Dosw. (Online).* **61:** 760–785.
13. Lund, E. G., T. A. Kerr, J. Sakai, W. P. Li, and D. W. Russell. 1998. cDNA cloning of mouse and human cholesterol 25-hydroxylases, polytopic membrane proteins that synthesize a potent oxysterol regulator of lipid metabolism. *J. Biol. Chem.* **273:** 34316–34327.
14. Bauman, D. R., A. D. Bitmansour, J. G. McDonald, B. M. Thompson, G. Liang, and D. W. Russell. 2009. 25-Hydroxycholesterol secreted by macrophages in response to Toll-like receptor activation suppresses immunoglobulin A production. *Proc. Natl. Acad. Sci. USA.* **106:** 16764–16769.
15. Diczfalusy, U., K. E. Olofsson, A. M. Carlsson, M. Gong, D. T. Golenbock, O. Rooyackers, U. Flaring, and H. Bjorkbacka. 2009. Marked upregulation of cholesterol 25-hydroxylase expression by lipopolysaccharide. *J. Lipid Res.* **50:** 2258–2264.
16. Lund, E., I. Björkhem, C. Furster, and K. Wikvall. 1993. 24-, 25- and 27-hydroxylation of cholesterol by a purified preparation of 27-hydroxylase from pig liver. *Biochim. Biophys. Acta.* **1166:** 177–182.
17. Li, X., W. M. Pandak, S. K. Erickson, Y. Ma, L. Yin, P. Hylemon, and S. Ren. 2007. Biosynthesis of the regulatory oxysterol, 5-cholesten-3β,25-diol 3-sulfate, in hepatocytes. *J. Lipid Res.* **48:** 2587–2596.
18. Lund, E. G., J. M. Guileyardo, and D. W. Russell. 1999. cDNA cloning of cholesterol 24-hydroxylase, a mediator of cholesterol homeostasis in the brain. *Proc. Natl. Acad. Sci. USA.* **96:** 7238–7243.
19. Smith, L. L. 1981. Cholesterol Autoxidation. Plenum Press, New York.
20. Honda, A., G. Salen, Y. Matsuzaki, A. K. Batta, G. Xu, E. Leitersdorf, G. S. Tint, S. K. Erickson, N. Tanaka, and S. Shefer. 2001. Differences in hepatic levels of intermediates in bile acid biosynthesis between Cyp27−/− mice and CTX. *J. Lipid Res.* **42:** 291–300.
21. Honda, A., G. Salen, Y. Matsuzaki, A. K. Batta, G. Xu, E. Leitersdorf, G. S. Tint, S. K. Erickson, N. Tanaka, and S. Shefer. 2001. Side chain hydroxylations in bile acid biosynthesis catalyzed by CYP3A are markedly up-regulated in Cyp27−/− mice but not in cerebrotendinous xanthomatosis. *J. Biol. Chem.* **276:** 34579–34585.
22. Kliewer, S. A., and T. M. Willson. 2002. Regulation of xenobiotic and bile acid metabolism by the nuclear pregnane X receptor. *J. Lipid Res.* **43:** 359–364.
23. Bodin, K., L. Bretillon, Y. Aden, L. Bertilsson, U. Broome, C. Einarsson, and U. Diczfalusy. 2001. Antiepileptic drugs increase plasma levels of 4β-hydroxycholesterol in humans: evidence for involvement of cytochrome p450 3A4. *J. Biol. Chem.* **276:** 38685–38689.
24. Diczfalusy, U., K. P. Kanebratt, E. Bredberg, T. B. Andersson, Y. Bottiger, and L. Bertilsson. 2008. 4β-Hydroxycholesterol as an endogenous marker for CYP3A4/5 activity. Stability and half-life of elimination after induction with rifampicin. *Br. J. Clin. Pharmacol.* **67:** 38–43.
25. Dzeletovic, S., O. Breuer, E. Lund, and U. Diczfalusy. 1995. Determination of cholesterol oxidation products in human plasma by isotope dilution-mass spectrometry. *Anal. Biochem.* **225:** 73–80.
26. Wu, J. C., G. Merlino, and N. Fausto. 1994. Establishment and characterization of differentiated, nontransformed hepatocyte cell lines derived from mice transgenic for transforming growth factor α. *Proc. Natl. Acad. Sci. USA.* **91:** 674–678.

27. Honda, A., K. Yamashita, H. Miyazaki, M. Shirai, T. Ikegami, G. Xu, M. Numazawa, T. Hara, and Y. Matsuzaki. 2008. Highly sensitive analysis of sterol profiles in human serum by LC-ESI-MS/MS. *J. Lipid Res.* **49:** 2063–2073.
28. Honda, A., K. Yamashita, T. Hara, T. Ikegami, T. Miyazaki, M. Shirai, G. Xu, M. Numazawa, and Y. Matsuzaki. 2009. Highly sensitive quantification of key regulatory oxysterols in biological samples by LC-ESI-MS/MS. *J. Lipid Res.* **50:** 350–357.
29. Honda, A., T. Miyazaki, T. Ikegami, J. Iwamoto, K. Yamashita, M. Numazawa, and Y. Matsuzaki. 2010. Highly sensitive and specific analysis of sterol profiles in biological samples by HPLC-ESI-MS/MS. *J. Steroid Biochem. Mol. Biol.* **121:** 556–564.
30. Ono, S., T. Hatanaka, H. Hotta, T. Satoh, F. J. Gonzalez, and M. Tsutsui. 1996. Specificity of substrate and inhibitor probes for cytochrome P450s: evaluation of in vitro metabolism using cDNA-expressed human P450s and human liver microsomes. *Xenobiotica.* **26:** 681–693.
31. Bodin, K., U. Andersson, E. Rystedt, E. Ellis, M. Norlin, I. Pikuleva, G. Eggertsen, I. Bjorkhem, and U. Diczfalusy. 2002. Metabolism of 4β-hydroxycholesterol in humans. *J. Biol. Chem.* **277:** 31534–31540.
32. Norlin, M., U. Andersson, I. Bjorkhem, and K. Wikvall. 2000. Oxysterol 7α-hydroxylase activity by cholesterol 7α-hydroxylase (CYP7A). *J. Biol. Chem.* **275:** 34046–34053.
33. Li-Hawkins, J., E. G. Lund, S. D. Turley, and D. W. Russell. 2000. Disruption of the oxysterol 7α-hydroxylase gene in mice. *J. Biol. Chem.* **275:** 16536–16542.
34. Guengerich, F. P. 1990. Mechanism-based inactivation of human liver microsomal cytochrome P-450 IIIA4 by gestodene. *Chem. Res. Toxicol.* **3:** 363–371.
35. Swell, L., C. C. Schwartz, J. Gustafsson, H. Danielsson, and Z. R. Vlahcevic. 1981. A quantitative evaluation of the conversion of 25-hydroxycholesterol to bile acids in man. *Biochim. Biophys. Acta.* **663:** 163–168.
36. Repa, J. J., E. G. Lund, J. D. Horton, E. Leitersdorf, D. W. Russell, J. M. Dietschy, and S. D. Turley. 2000. Disruption of the sterol 27-hydroxylase gene in mice results in hepatomegaly and hypertriglyceridemia. *J. Biol. Chem.* **275:** 39685–39692.
37. Honda, A., G. Salen, Y. Matsuzaki, A. K. Batta, G. Xu, T. Hirayama, G. S. Tint, M. Doy, and S. Shefer. 2005. Disrupted coordinate regulation of farnesoid X receptor target genes in a patient with cerebrotendinous xanthomatosis. *J. Lipid Res.* **46:** 287–296.

Impact of Ovarian Sex Steroids on Ovulation and Ovulatory Gene Induction in Aromatase-Null Mice

Katsumi Toda, Yoshihiro Hayashi, Masafumi Ono, and Toshiji Saibara

Departments of Biochemistry (K.T.), Pathology (Y.H.), and Gastroenterology and Hepatology (M.O., T.S.), Kochi University, School of Medicine, Nankoku, Kochi 783-8505, Japan

Female mice deficient in the aromatase gene [aromatase knockout (ArKO)] fail to ovulate owing to an inability to produce estrogens. Here, we demonstrated that sequential administration of adequate amounts of 17β-estradiol (E2), pregnant mare serum gonadotropin, and human chorionic gonadotropin could induce ovulation in immature ArKO mice; nevertheless, significantly fewer oocytes were released into the oviducts in ArKO mice than in wild-type mice. Analysis of ovarian steroids by liquid chromatography coupled with electrospray ionization-tandem mass spectrometry identified a trace amount of E2 in the untreated immature ArKO ovary. The analysis further detected significant increases and decreases in progesterone and testosterone contents, respectively, in addition to an increase of E2 in the ovulation-induced ArKO ovaries compared with the levels in untreated ArKO ovaries. Gene expression analysis demonstrated marked elevation in the mRNA levels of members of the epidermal growth factor family and extracellular matrix-related proteins at 4 h after human chorionic gonadotropin injection in the ovaries of ArKO mice treated for ovulation, as observed in the ovulation-induced wild-type ovaries. Collectively, these findings suggest the vital contribution of the intraovarian milieu of sex steroids to ovulatory regulation *in vivo*. (***Endocrinology*** **153: 386–394, 2012)**

Estrogens are important in the regulation of female reproductive functions. Negative and positive feedback regulations on GnRH and gonadotropin secretion in particular are critical for the physiological control of ovulatory cycling (1). In addition, considerable studies have been carried out to demonstrate the roles of estrogens in folliculogenesis, steroidogenesis, ovulation, and corpus luteum formation (2–5). However, it is still unclear which ovarian responses triggered by gonadotropins are estrogen-dependent, because the ovary is the site of synthesis of estrogens in response to gonadotropins.

Conversion of androgens to estrogens is catalyzed by the enzyme called aromatase, which is encoded by the genomic gene termed *Cyp19a1* (6). Targeted disruption of *Cyp19a1* in female mouse [aromatase knockout (ArKO) mouse] resulted in complete infertility due to estrogen insufficiency (7, 8). Because ArKO mice enable us to distinguish between estrogen dependent and independent events triggered by gonadotropins in ovarian tissue, various histological and physiological studies have been intensively conducted (6–10). Histological analyses of ArKO ovaries revealed follicular depletion at early developmental stages and extensive formation of hemorrhage (7–9). Physiological studies demonstrated that ArKO females ovulate neither spontaneously nor artificially after administration of ovulatory doses of gonadotropins (8–11). The anovulatory phenotype of ArKO females was recovered from by surgical replacement of their ovaries with wild-type (WT) ovaries. Consequently, the mice became fertile (11). These studies suggested that ovarian dysfunction is the primary cause of the infertility of ArKO females. To date, any trials to induce ovulation by supplementing ArKO mice with exogenous 17β-estradiol (E2) have been unsuccessful (8, 12), implying that deletion of *Cyp19a1* might cause irreversible alternations in ovarian physiology essential for ovulatory induction. In addition, inability to induce ovu-

ISSN Print 0013-7227 ISSN Online 1945-7170
Printed in U.S.A.

doi: 10.1210/en.2011-1462 Received July 6, 2011. Accepted November 2, 2011.
First Published Online December 6, 2011

Abbreviations: ArKO, Aromatase knockout; COC, cumulus-oocyte complex; DHT, dihydrotestosterone; E2, 17β-estradiol; EGF, epidermal growth factor; hCG, human chorionic gonadotropin; LC-MS/MS, liquid chromatography-electrospray ionization tandem mass spectrometry; P4, progesterone; PMSG, pregnant mare serum gonadotropin; RT-QPCR, real-time quantitative PCR; T, testosterone; WT, wild type.

lation with supplementation of E2 and gonadotropins might indicate involvement of unknown factors vital for ovulatory induction of the estrogen-deficient mice.

In this study, with the aim of elucidating the underlying causes of the infertility due to estrogen insufficiency, we attempted to establish a superovulation regimen for ArKO females. Our morphological and biochemical analysis demonstrated that ovulation could be induced in ArKO mice when stimulated the ovary with E2 and gonadotropins in an sequential manner appropriately, emphasizing that the anovulatory phenotype is reversible. Furthermore, present superovulation regimen for ArKO females will provide a way to determine the relative contribution of E2 and gonadotropins to the molecular events immediately preceding ovulation.

Materials and Methods

Animals and treatments

Animal experiments were carried out according to the Guidelines for the Care and Treatment of Laboratory Animals of Kochi University. Treatments of WT and ArKO mice (8, 13) were summarized in Table 1. Pregnant mare serum gonadotropin (PMSG) and human chorionic gonadotropin (hCG) were respectively obtained from ASKA Pharmaceutical Co., Ltd. (Tokyo and Wako Pure Chemical Industries, Osaka, Japan). E2 (minimum purity 98%; Sigma-Aldrich Corp., St. Louis, MO) dissolved at 0.15 or 1.5 mg/ml in sesame oil was sc administrated to ArKO mice. Numbers of released cumulus-oocyte complexes (COC) were determined by oviductal inspection at 15 h after hCG injection.

In vitro fertilization

In vitro fertilization experiments were conducted to assess the physiological quality of ArKO oocytes (see Supplemental Materials and Methods, published on The Endocrine Society's Journals Online web site at http://endo.endojournals.org).

RNA preparation and real-time quantitative PCR (RT-QPCR) analysis

Ovaries from nine to ten mice were pooled (n = 3) and used for RNA preparation. Conditions for RNA preparation, cDNA synthesis, and RT-QPCR (Supplemental Fig. 1) were detailed in Supplemental Materials and Methods. Primer sequences are presented in Supplemental Table 1.

Histological examination and immunohistochemistry

Ovaries were removed from the mice, fixed in a 10% (vt/vt) buffered formalin solution, and embedded in paraffin. The sections at 3-μm thickness were stained with hematoxylin and eosin or with an antibody against cytochrome P450scc (Santa Cruz Biotechnology, Inc., Santa Cruz, CA) according to the manufacturer's instructions.

Ovarian steroid contents

Because E2 contents were expected to be at a negligible level in ArKO mice, ovaries from four to 10 mice dependent on the genotype and treatment were pooled (n = 2). Ovarian contents of progesterone (P4), testosterone (T), dihydrotestosterone

TABLE 1. Summary for animal treatment

Experimental group	Genotype	Treatment				Ovary collected at
		Day 1	Day 4	Day 5	Day 6	
1	WT		Without treatment			
2	WT		PMSG (5)			0
3	WT		PMSG (5)		hCG (5)	4
4	WT		PMSG (5)		hCG (5)	15
5	WT	E2	E2/PMSG (25)	E2	hCG (25)	15
6	ArKO		Without treatment			
7	ArKO	E2	E2	E2		0
8	ArKO		PMSG (25)			0
9	ArKO	E2	E2/PMSG (25)	E2		0
10	ArKO	E2	E2/PMSG (5)	E2		0
11	ArKO		PMSG (25)		hCG (25)	4
12	ArKO	E2	E2/PMSG (25)	E2	hCG (25)	4
13	ArKO	E2	E2/PMSG (5)	E2	hCG (5)	4
14	ArKO		PMSG (25)		hCG (25)	15
15	ArKO	E2	E2/PMSG (25)	E2	hCG (25)	15
16	ArKO	E2	E2/PMSG (5)	E2	hCG (5)	15
17	ArKO	E2[a]	E2[a]/PMSG (25)	E2[a]	hCG (25)	15

Immature WT mice at 4 wk of age were injected ip with 5 IU of PMSG on d 4 followed 48 h later with 5 IU of hCG on d 6 to promote synchronized follicle growth and ovulation. ArKO mice were stimulated with E2 on d 1, 4, and 5 (10 mg/kg BW, sc injection), PMSG on d 4 (25 or 5 IU/mouse), and hCG on d 6 (25 or 5 IU/mouse). Ovaries were collected at follicular growth stage as indicated by 0 (48 h after PMSG injection for mice treated with PMSG alone or 24 h after the last injection of E2 for mice treated with E2 alone or E2 plus PMSG), at preovulatory differentiation stage as indicated by 4 (4 h after hCG injection), and after ovulation as indicated by 15 (15 h after hCG injection). BW, Body weight.

[a] ArKO mice were supplemented with E2 at 1 mg/kg BW (group 17).

(DHT), and E2 in the pooled samples were measured in triplicate by liquid chromatography-electrospray ionization tandem mass spectrometry (LC-MS/MS) (Supplemental Materials and Methods). Detection limits for P4, T, DHT, and E2 are 2, 1, 1, and 0.5 pg per assay, respectively (14). Contents of each steroid were expressed as amounts of steroid per milligram of ovarian wet weight from three independent measurements.

Western blot analyses

Pooled ovaries from five mice per group (n = 3) were sonicated in 100 μl of 50 mM Tris-HCl (pH 7.4) containing 0.1 mM EDTA, 0.1 mM EGTA, 0.1% sodium dodecyl sulfate, protease inhibitor cocktail (Roche Diagonostics GmbH, Munich, Germany) and phosphatase inhibitor cocktail (Pierce, Rockford, IL). The sonicated samples were further homogenized using the Bio-Masher extraction device (Omni International, Kennesaw, GA). After centrifugation at 16,000 × *g* for 10 min at 4 C, the supernatants were used as total ovarian extracts for Western blot analysis. Protein concentrations were quantified using a bicinchoninic acid protein assay kit (Thermo Scientific, Rockford, IL). Methods of Western blot analysis were detailed in Supplemental Materials and Methods.

Statistical analysis

Continuous variables were expressed in mean ± SE. Mann-Whitney *U* test and *t* test were used for analysis when they were applicable (InStat software; GraphPad Software, Inc., San Diego, CA). *P* values less than 0.05 were considered significant.

Results

Recovery from anovulatory phenotype in *ArKO* mouse

WT females treated with E2 plus 25 IU of PMSG followed by 25 IU of hCG ovulated significantly fewer oocytes per animal than those after a conventional superovulation regimen composed of 5 IU of PMSG and hCG (14.1 ± 2.4 *vs.* 27.3 ± 2.5 oocytes/mouse, $P < 0.001$) (Table 2). In contrast to WT mice, none of the ArKO mice ovulated upon the treatment with high doses of gonadotropin stimulation alone or conventional doses of gonadotropins with E2 supplementation (Table 2). However, treatment of ArKO mice with E2 plus 25 IU of PMSG followed by 25 IU of hCG restored the anovulatory phenotype (Fig. 1A). Ovulatory response was observed in 42 of 60 ArKO mice examined, although the numbers of oocytes released into the oviducts were significantly fewer than those in WT mice (6.9 ± 0.9 *vs.* 27.3 ± 2.5 oocytes/mouse, $P < 0.001$) (Table 2). When ArKO mice were treated with a low dose of E2, ovulation was observed in only one mouse out of 13 ArKO mice examined. Morphological analyses of the released oocytes in the oviducts showed no major abnormalities. In addition, the oocytes recovered from the oviducts could fertilize with sperm from matured WT mouse *in vitro*, excluding a possible global defect in the quality of ovulated ArKO oocytes (Fig. 1B). In support of ovulatory induction in ArKO mice, staining of the ArKO ovary with polyclonal P450scc antibody revealed strong positive signals, indicating differentiation of granulosa cells into luteal cells (Fig. 1C).

Alterations in sex steroid contents after ovulatory stimulation in ArKO ovaries

We next examined ovarian contents of P4, T, DHT, and E2 using LC-MS/MS at various ovarian stages (Table 3). The contents of P4 in the ovary of WT mice were 1.35 and 1.45 ng/mg without treatment and after the treatment with PMSG, respectively. E2 content in the ovary of WT mice without treatment was 6.01 pg/mg, which was nearly equivalent to the level of adult WT mice at a diestrous stage when analyzed by LC-MS/MS assay (4.9 pg/mg) (15). When stimulated with PMSG, E2 content significantly increased to 134 pg/mg in WT mice ($P < 0.001$). The contents of T and DHT also increased by 32- and 7-fold, respectively, compared with the untreated WT levels ($P < 0.001$ and $P < 0.001$, respectively).

In the ovary of untreated ArKO mice, P4 content was only 6% of the untreated WT levels ($P < 0.001$), whereas T and DHT contents were higher than those in the WT ovaries ($P < 0.001$ and $P < 0.001$, respectively); in particular, the former was 30-fold over the untreated WT levels. Unexpectedly, a trace amount of E2 (0.05 pg/mg) was detected in the ovary of the untreated ArKO mice

TABLE 2. Summary of ovulatory induction in ArKO mice

Genotype	Experimental group	E2 (mg/kg)	PMSG[a] (IU)	hCG (IU)	Mice showing ovulation (%)	No. of ovulated COC/mouse
WT (*n* = 23)	4		5	5	23 (100)	27.3 ± 2.5
WT (*n* = 14)	5	10	25	25	13 (92)	14.1 ± 2.4[a]
ArKO (*n* = 15)	14		25	25	0	0
ArKO (*n* = 60)	15	10	25	25	42 (70)	6.9 ± 0.9[a]
ArKO (*n* = 9)	16	10	5	5	0	0
ArKO (*n* = 13)	17	1	25	25	1 (8)	2

E2, 1 or 10 mg/kg BW sc at d 1, 4, and 5. PMSG, 5 or 25 IU/mouse at d 4. hCG, 5 or 25 IU at d 6. No. of ovulated COC/mouse, Average COC numbers per mouse showing ovulation. Nos. in the experimental group *column* correspond to those in Table 1. BW, Body weight.

[a] $P < 0.001$ *vs.* WT mice treated with 5 IU of gonadotropins (group 4).

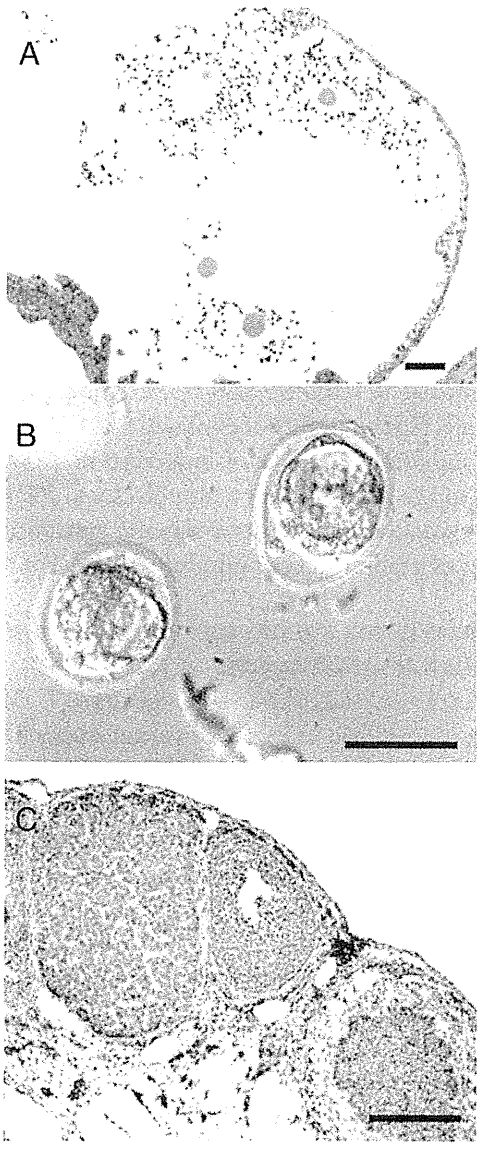

FIG. 1. Ovulatory induction in ArKO mouse. A, Sections of the oviduct of ArKO mouse at 15 h after hCG injection were stained with hematoxylin and eosin. *Scale bar*, 200 μm. B, Ovulated oocytes of ArKO mice were collected from the oviducts and used for *in vitro* fertilization with sperm from WT mouse. The light microscope image of fertilized oocytes at d 5 after incubation with the sperm was presented. *Scale bar*, 50 μm. C, Sections of the ovary from ArKO mice at 15 h after hCG injection were stained with an antibody against P450scc. *Scale bar*, 200 μm.

under the present assay conditions (Supplemental Fig. 2). As expected, ovarian E2 content was increased significantly by exogenous supplementation with E2 (9.7 and 9.9 pg/mg with E2 alone and with E2 plus PMSG, respectively) ($P < 0.001$ and $P < 0.001$ *vs.* untreated ArKO ovaries, respectively); nevertheless, the contents were around the range of the untreated WT levels. Treatment with PMSG alone increased P4 content 1.5-fold over the untreated ArKO levels ($P < 0.001$), whereas it had marginal effects on T and DHT in ArKO mice (not significant and $P < 0.04$, respectively). E2 treatment also caused a 3-fold increase in P4 content ($P < 0.001$), but it markedly decreased in T and DHT contents: 2.8 and 20% of the untreated ArKO levels, respectively ($P < 0.001$ and $P < 0.001$, respectively). When ArKO mice were treated with E2 plus PMSG, P4 increased 8-fold, but T and DHT decreased to 28 and 14%, respectively, compared with those of untreated ArKO mice ($P < 0.001$, $P < 0.001$, and $P < 0.001$, respectively).

P4 content in the WT ovary at the preovulatory differentiation stage was increased 2.3-fold, but T, DHT, and E2 decreased to 22, 11, and 26%, respectively, of the WT levels at the follicular growth stage ($P < 0.001$, $P < 0.001$, $P < 0.001$, and $P < 0.001$, respectively). P4 in the ArKO ovary at this stage was 2.3 ng/mg, which was similar to the ovary of ArKO mice after treatment with E2 plus 5 IU of gonadotropins (nonovulatory dose for ArKO mouse) (Table 2). T, DHT, and E2 decreased in ArKO ovary at preovulatory differentiation stage to 22, 41, and 25% of the ArKO levels at the follicular growth stage, respectively ($P < 0.001$, $P < 0.001$, and $P < 0.001$, respectively), as observed in the WT ovary. In the ArKO ovary stimulated with nonovulatory dose of hCG (5 IU/mouse), DHT and E2 contents decreased to 43 and 53% of the ArKO levels at the follicular growth stage, respectively ($P < 0.001$ and $P < 0.001$, respectively), whereas relatively high T content compared with that in the ArKO ovary stimulated with ovulatory dose of hCG (25 IU/mouse) ($P < 0.001$) was detected, which was approximately a half of the untreated ArKO level.

P4 content in the ovulated WT ovary was 3.2 ng/mg, nearly same contents as those at the preovulatory differentiation stage ($P = 0.053$). In contrast, T, DHT, and E2 contents decreased, reaching approximately the untreated WT levels ($P < 0.001$, $P < 0.001$, and $P < 0.001$, respectively). Content of E2 in the ovulated ArKO ovary decreased by 48% of that of ArKO ovary of the preovulatory differentiation stage ($P < 0.001$), whereas the other three steroids did not change significantly ($P = 0.07$, $P = 0.20$, and $P = 0.16$, respectively). The ovaries of ArKO mice treated with high doses of gonadotropins alone showed a low level of P4 with high levels of T and DHT, as observed in the untreated ArKO ovaries.

Gene expression analysis

The effects of the current superovulation regimen on transcript levels of a subset of genes related with ovulation were evaluated by RT-QPCR analysis.

At the follicular growth stage (Fig. 2), mRNA expression of *Fshr* and *Lhcgr* was up-regulated after PMSG treatment in the WT ovaries ($P < 0.01$ and $P < 0.001$) (Fig. 2, experimental group 2): 1.5- and 16-fold over the untreated

TABLE 3. Ovarian steroids

Experimental group		P4 (ng/mg)	T (pg/mg)	DHT (pg/mg)	E2 (pg/mg)	T/E2
WT						
1	Without treatment	1.35 ± 0.18	14.3 ± 4.2	2.10 ± 0.22	6.01 ± 0.68	2.4
ArKO						
6	Without treatment	0.08 ± 0.02[a]	433.0 ± 13.5[a]	7.51 ± 0.8[a]	0.05 ± 0.01[a]	8660
At follicular growth stage (48 h after PMSG injection)						
WT						
2	With P	1.45 ± 0.23	471.0 ± 53.5[a]	15.8 ± 1.89[a]	134.7 ± 2.56[a]	3.5
ArKO						
9	With E2P	0.69 ± 0.07[b]	124.1 ± 15.5[b]	1.05 ± 0.11[b]	9.9 ± 1.14[b]	12.5
7	With E2	0.24 ± 0.03[b]	12.2 ± 3.04[b]	1.52 ± 0.16[b]	9.7 ± 1.10[b]	1.3
8	With P	0.12 ± 0.02[b]	467.0 ± 81.2[c]	10.7 ± 1.23[d]	0.04 ± 0.01[d]	11675
At preovulatory differentiation stage (4 h after hCG injection)						
WT						
3	With Ph	3.38 ± 0.4[e]	105.6 ± 11.7[e]	1.71 ± 0.20[e]	35.4 ± 4.39[e]	3.0
ArKO						
12	With E2Ph	2.34 ± 0.25	27.2 ± 5.43[f]	0.43 ± 0.05[f]	2.52 ± 0.27[f]	10.8
13	With E2Ph (5 IU)	2.87 ± 0.44	203.6 ± 31.3[g]	0.45 ± 0.06[f]	5.22 ± 0.59[f]	39.0
After ovulation (15 h after hCG injection)						
WT						
4	With Ph	3.15 ± 0.34[h]	10.0 ± 1.9[i]	0.79 ± 0.0[i]	3.56 ± 0.44[i]	2.8
ArKO						
15	With E2Ph	1.81 ± 0.15	18.1 ± 4.8	30.35 ± 0.03	1.31 ± 0.15[g]	13.8
14	With Ph (No ovulation)	0.13 ± 0.01	206.2 ± 29.5	4.6 ± 0.15	0.02 ± 0.004	10300

Ovaries of WT mice and ArKO mice supplemented with hormones were collected and analyzed for steroid hormone contents by means of LC-MS/MS. The contents were expressed as a basis of ovarian wet weigh (mg) (mean ± SEM). Numbers of experimental groups in Table 1 were presented. E2P, E2 plus PMSG; E2Ph, E2 plus PMSG plus hCG; h, hCG; P, PMSG; Ph, PMSG plus hCG.

[a] $P < 0.001$, *vs.* WT mice without treatment (group 1).

[b] $P < 0.001$, *vs.* ArKO mice without treatment (group 6).

[c] Not significant *vs.* ArKO mice without treatment (group 6).

[d] $P < 0.04$, *vs.* ArKO mice without treatment (group 6).

[e] $P < 0.001$, *vs.* WT mice with P (group 2).

[f] $P < 0.001$, *vs.* ArKO mice with E2P (group 9).

[g] $P < 0.001$, *vs.* ArKO mice with E2Ph (group 12).

[h] $P = 0.053$, *vs.* WT mice after 4 h with Ph (group 3).

[i] $P < 0.001$, *vs.* WT mice after 4 h with Ph (group 3).

WT levels (Fig. 2, group 1), respectively, whereas that of *Pgr* remained unchanged. The levels of *Lhcgr* and *Pgr* in the ArKO ovaries were significantly suppressed to 36 and 18% of the untreated WT levels, respectively ($P < 0.001$ and $P < 0.001$) (Fig. 2, group 6). Treatment of ArKO mice with E2 significantly increased the expression of *Lhcgr* and *Pgr* by 4- and 8.4-fold over the untreated level ($P < 0.001$ and $P < 0.001$), respectively (Fig. 2, group 7). Treatment of ArKO mice with PMSG alone (Fig. 2, group 8) caused 1.6-fold increase in Fshr mRNA levels ($P < 0.02$) but had no effect on the *Lhcgr* and *Pgr* mRNA expression. In contrast, the *Lhcgr* expression was increased by the treatment with E2 plus PMSG (Fig. 2, group 9), 28-fold over the untreated ArKO level ($P < 0.001$), whereas the mRNA expression levels of *Fshr* and *Pgr* after treatment with E2 plus PMSG were nearly the same as those observed in the ovary treated with PMSG alone. No significant difference in *Fshr*, *Lhcgr*, and *Pgr* mRNA expression levels was observed in the ArKO mice between treatment with E2 plus high and low doses of PMSG (Fig. 2, groups 9 and 10).

Next, the mRNA levels of genes specifically induced at the preovulatory differentiation stage were examined (Fig. 3) (16–18). Significant elevations in the mRNA expression levels of all the genes shown in Fig. 3 were confirmed in the WT ovaries ($P < 0.001$) (Fig. 3, group 3). The expression levels of both *Lhcgr* and *Pgr* mRNA were significantly increased by the treatment with E2 plus

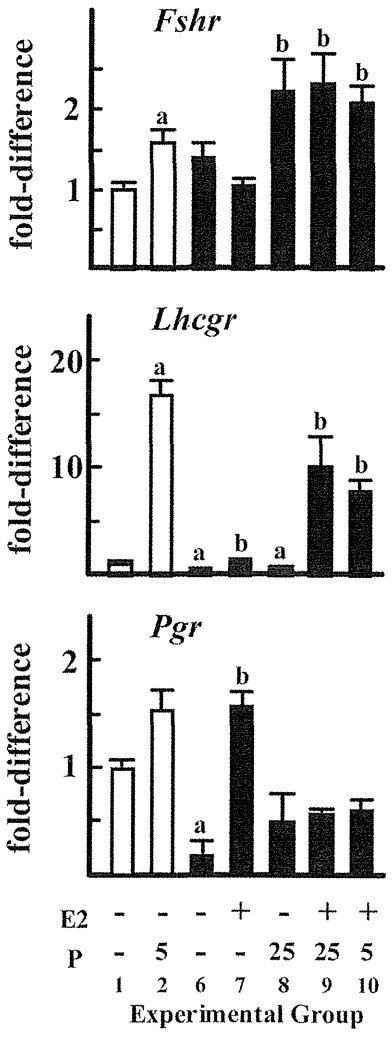

FIG. 2. RT-QPCR analysis of the ovarian mRNA expressions at follicular growth stage. WT (*open bar*) and ArKO (*closed bar*) mice were treated according to the schedule shown in Table 1 (9–12 mice per group, n = 3). *Bar* illustrates fold difference compared with the expression level in WT ovaries without treatment (mean ± SEM). E2, 10 mg/kg body weight. P, PMSG; *numeral*, dosage (IU)/mouse. Numbers for experimental groups presented in Table 1 were marked under the graphs. a, $P < 0.05$ against untreated WT levels (group 1); b, $P < 0.05$ against untreated ArKO levels (group 6). The absence of *letters* on a *bar* indicates that difference does not reach significance statistically. Exp, Experimental.

gonadotropins in ArKO mice ($P < 0.02$ and $P < 0.001$) (Fig. 3, group 12); nevertheless, the latter level was half of the WT level at this stage ($P < 0.02$). In the ovulated ovaries in WT and ArKO mice (Fig. 3, groups 4 and 15), *Lhcgr* mRNA expression levels remained high, whereas the level of *Pgr* became noticeably low ($P < 0.001$). Marked induction of the mRNA expression for epidermal growth factor (EGF)-like growth factors, including *Areg*, *Btc*, and *Ereg*, was observed in ArKO ovaries at the preovulatory differentiation stage (group 12) ($P < 0.001$, $P < 0.001$, and $P < 0.001$); nevertheless, the magnitude of the induction of *Areg* and *Ereg* mRNA expression was less than the WT levels ($P < 0.001$ and $P < 0.001$). Notably, no marked up-regulation of these mRNA expressions was observed in the ArKO ovaries without E2 supplementation (Fig. 3, groups 11 and 14). Likewise, mRNA expression levels of factors controlling COC expansion, including *Ptgs2*, *Has2*, *Ptx3*, *Tmfaip6*, and *Vcan*, were significantly increased by the ovulatory stimulation ($P < 0.001$, $P < 0.001$, $P < 0.001$, $P < 0.001$, and $P < 0.02$, respectively) (Fig. 3, group 12). Furthermore, expressions of these genes except for *Ptx3* and *Has2* were significantly up-regulated in untreated ArKO ovaries (*Ptgs2*, $P < 0.01$; *Tmfaip6*, $P < 0.001$; and *Vcan*, $P < 0.01$, respectively) (Fig. 3, group 6), and they were enhanced by treatment with gonadotropin alone (Fig. 3, groups 11 and 14) (*Ptgs2*, $P < 0.001$; *Ptx3*, $P < 0.001$; and *Tmfaip6*, $P < 0.001$, respectively). In the ovulated ovaries of WT and ArKO mice, the mRNA levels of EGF-like and COC-related factors except for *Vcan* in WT mice showed a clear decline ($P < 0.001$) (Fig. 3, groups 4 and 15). In summary, the present RT-QPCR analysis demonstrated that the ovulatory regimen for ArKO mice increased mRNA levels of genes encoding factors critical for the ovulatory process; nevertheless, the expression of some genes, such as *Pgr*, *Areg*, *Ereg*, *Has2*, and *Ptx3*, was enhanced less markedly in ArKO ovaries than in WT ovaries ($P < 0.001$, $P < 0.001$, and $P < 0.001$, respectively).

Next, the transcript levels in the ovary of ArKO mice treated with E2 plus 5 IU of gonadotropins (nonovulatory dose) (Table 2) were compared with those in the ovary treated with the current superovulation regimen (Fig. 3, groups 12 and 13). The mRNA levels for EGF-like growth factors and COC-related proteins in the ovary treated with nonovulatory stimulations were nearly equal to the levels in the ovary treated for ovulation. However, significant differences in the expression levels between ovulatory and nonovulatory stimulations were detected in the Lhcgr, Pgr, and Btc mRNA expressions ($P < 0.01$, $P < 0.001$, and $P < 0.001$, respectively). The lower mRNA levels of Lhcgr expression might be related to less efficient luteinization in the ovary treated with a low dose of gonadotropins.

Induction of ERK1/2 phosphorylation by ovulatory stimulation in ArKO mice

Several lines of evidence indicate that transduction of the EGFR signaling is essential for LH-induced ovulation process (18–21). Thus, we examined the phosphorylated ERK1/2 levels in ArKO mice after ovulatory stimulation (Fig. 4). As expected, stimulation with hCG increased ERK1/2 phosphorylation in the ovary of PMSG-primed WT mice (group 3, $P < 0.001$ *vs.* group 1, $P < 0.01$ *vs.* group 2) (Fig. 4). In untreated ArKO ovary, the basal phosphorylation levels of ERK1/2 were 3-fold higher than